Cell Metabolism
Clinical and Translational Report

Effects on weight loss and glycemic control with SAR441255, a potent unimolecular peptide GLP-1/GIP/GCG receptor triagonist

Graphical abstract

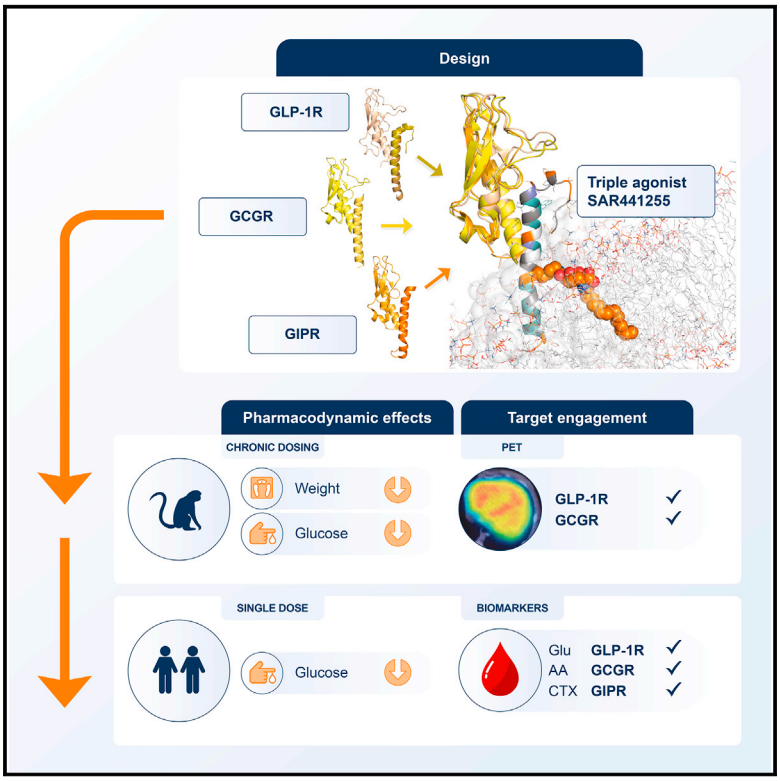

Highlights

- SAR441255 showed substantial body weight loss in diabetic obese monkeys
- SAR441255 also improved glucose control in diabetic obese monkeys
- PET imaging in monkeys confirmed high receptor occupancy with SAR441255
- In healthy subjects, biomarkers confirmed simultaneous SAR441255 receptor engagement

Authors

Martin Bossart, Michael Wagner, Ralf Elvert, ..., William B. Smith, Almut Nitsche, Anish Konkar

Correspondence

martin.bossart@sanofi.com (M.B.), konkar_anish@lilly.com (A.K.)

In brief

Bossart et al. designed a unimolecular triple GLP-1R/GCGR/GIPR agonist with substantial metabolic activity in preclinical animal models. In a single-dose study in human subjects, SAR441255 lowered plasma glucose during a mixed-meal tolerance test with a decrease in plasma biomarker levels supportive of engagement at all three targeted receptors.

Bossart et al., 2022, Cell Metabolism *34*, 59–74
January 4, 2022
https://doi.org/10.1016/j.cmet.2021.12.005

CellPress

Cell Metabolism

CellPress
OPEN ACCESS

Clinical and Translational Report

Effects on weight loss and glycemic control with SAR441255, a potent unimolecular peptide GLP-1/GIP/GCG receptor triagonist

Martin Bossart,[1,17,*] Michael Wagner,[1,12] Ralf Elvert,[2,13] Andreas Evers,[1,14] Thomas Hübschle,[2] Tim Kloeckener,[2,15] Katrin Lorenz,[1] Christine Moessinger,[2] Olof Eriksson,[3,4] Irina Velikyan,[4,5] Stefan Pierrou,[3] Lars Johansson,[3] Gabriele Dietert,[6] Yasmin Dietz-Baum,[6] Thomas Kissner,[6] Irene Nowotny,[7] Christine Einig,[8] Christelle Jan,[9] Faiza Rharbaoui,[7] Johann Gassenhuber,[7] Hans-Peter Prochnow,[7] Inoncent Agueusop,[8] Niels Porksen,[10] William B. Smith,[11] Almut Nitsche,[10] and Anish Konkar[2,16,*]

[1]Synthetic Medicinal Modalities, Integrated Drug Discovery Germany, Sanofi, Frankfurt, Germany
[2]TA Diabetes, Sanofi, Frankfurt, Germany
[3]Antaros Medical AB, Mölndal, Sweden
[4]Science For Life Laboratory, Department of Medicinal Chemistry, Uppsala University, Uppsala, Sweden
[5]PET Centre, Centre for Medical Imaging, Uppsala University Hospital, Uppsala, Sweden
[6]Preclinical Safety, Sanofi, Frankfurt, Germany
[7]Translational Medicine & Early Development, Sanofi, Frankfurt, Germany
[8]Clinical Sciences & Operations, Sanofi, Frankfurt, Germany
[9]Clinical Sciences & Operations, Sanofi, Chilly-Mazarin, France
[10]Diabetes Development, Sanofi, Frankfurt, Germany
[11]NOCCR Alliance for Multispecialty Research (AMR), Knoxville, TN, USA
[12]Present address: Dewpoint Therapeutics, Frankfurt, Germany
[13]Present address: Evotec International GmbH, Goettingen, Germany
[14]Present address: Global Research & Development, Discovery Technologies, Merck Healthcare KGaA, Darmstadt, Germany
[15]Present address: Cardiometabolic Disease Research, Boehringer Ingelheim Pharma GmbH, Biberach/Riss, Germany
[16]Present address: Diabetes and Complications Therapeutic Area, Lilly Research Laboratories, Eli Lilly and Company, Indianapolis, IN, USA
[17]Lead contact
*Correspondence: martin.bossart@sanofi.com (M.B.), konkar_anish@lilly.com (A.K.)
https://doi.org/10.1016/j.cmet.2021.12.005

SUMMARY

Unimolecular triple incretins, combining the activity of glucagon-like peptide-1 (GLP-1), glucose-dependent insulinotropic polypeptide (GIP), and glucagon (GCG), have demonstrated reduction in body weight and improved glucose control in rodent models. We developed SAR441255, a synthetic peptide agonist of the GLP-1, GCG, and GIP receptors, structurally based on the exendin-4 sequence. SAR441255 displays high potency with balanced activation of all three target receptors. In animal models, metabolic outcomes were superior to results with a dual GLP-1/GCG receptor agonist. Preclinical *in vivo* positron emission tomography imaging demonstrated SAR441255 binding to GLP-1 and GCG receptors. In healthy subjects, SAR441255 improved glycemic control during a mixed-meal tolerance test and impacted biomarkers for GCG and GIP receptor activation. Single doses of SAR441255 were well tolerated. The results demonstrate that integrating GIP activity into dual GLP-1 and GCG receptor agonism provides improved effects on weight loss and glycemic control while buffering the diabetogenic risk of chronic GCG receptor agonism.

INTRODUCTION

The twin epidemics of type 2 diabetes (T2D) and obesity are a global health burden. Despite advice to manage their disease by increasing physical activity, maintaining a strict diet, and use available pharmacotherapy, many patients struggle to manage T2D and/or obesity (Upadhyay et al., 2018; Zaykov et al., 2016). At present, glucagon-like peptide 1 receptor agonists (GLP-1RAs) are the only approved class of drugs to have shown the potential to effectively treat both T2D and obesity (Nauck et al., 2021). In view of their significant and sustained effects on weight loss as well as favorable metabolic effects, GLP-1RAs are also being evaluated for the treatment of non-alcoholic fatty liver disease (NAFLD)/non-alcoholic steatohepatitis (NASH) (Seghieri et al., 2018; Sumida et al., 2020; Vilar-Gomez et al., 2015), an obesity-related condition for which there

A

Name	1	2	3	4	5	6	7	8	9	10	11	12	13	14	15	16	17	18	19	20	21	22	23	24	25	26	27	28	29	30	31	32	33	34	35	36	37	38	39	40	41	42	C-terminus
GLP-1(7-36)NH_2	H	A	E	G	T	F	T	S	D	V	S	S	Y	L	E	G	Q	A	A	K	E	F	I	A	W	L	V	K	G	R													NH_2
Exendin-4	H	G	E	G	T	F	T	S	D	L	S	K	Q	M	E	E	E	A	V	R	L	F	I	E	W	L	K	N	G	G	P	S	S	G	A	P	P	P	S				NH_2
Glucagon	H	S	Q	G	T	F	T	S	D	Y	S	K	Y	L	D	S	R	R	A	Q	D	F	V	Q	W	L	M	N	T															OH
GIP(1-42)	Y	A	E	G	T	F	I	S	D	Y	S	I	A	M	D	K	I	H	Q	Q	D	F	V	N	W	L	L	A	Q	K	G	K	K	N	D	W	K	H	N	I	T	Q	OH
SAR441255	H	Aib	H	G	T	F	T	S	D	L	S	K	L	K(γGlu-γGlu-Palm)	E	E	Q	R	Q	Aib	E	F	I	E	W	L	K	A	dAla	G	P	P	S	Aib	K	P	P	P	K				NH_2

B

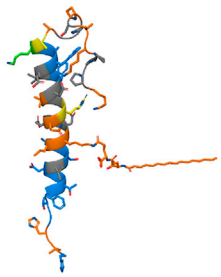

C

Recombinant receptor	Compound	Geometric mean EC_{50} (pM)	n
GLP-1	SAR441255	1.03	4
	GLP-1(7-36)NH_2	1.02	4
GCG	SAR441255	1.01	4
	Glucagon	0.47	4
GIP	SAR441255	0.73	4
	GIP(1-42)	0.33	4

D

Species	Cell line (receptor)	Compound	Geometric mean EC_{50} (pM)	n
Human	1.1B4 (GLP-1)	SAR441255	27	4
		GLP-1(7-36)NH_2	29	4
	Primary hepatocytes (GCG)	SAR441255	2100	4
		Glucagon	3000	4
	Adipocytes (GIP)	SAR441255	42	3
		GIP(1-42)	102	6

Figure 1. SAR441255 is a potent and balanced agonist of the GLP-1, GIP, and GCG receptors

(A) Amino acid (AA) sequences of GLP-1(7-36)NH_2, exendin-4, glucagon (GCG), GIP, and SAR441255. AAs that are identical between GCG and exendin-4 are colored blue, residues unique to exendin-4 are colored gray, residues unique to GCG are shown in yellow, residues unique to GLP-1 are shown in white, and residues unique to GIP are shown in purple. Additional modifications introduced to enhance selectivity or metabolic stability are shown in orange.

(B) Modeling hypothesis of the SAR441255 3D structure in the conformation binding to the GLP-1, GIP, and GCG receptor. The color coding of peptide AAs is equivalent to the sequence color coding outlined in (A).

(C) Agonist potencies (mean apparent 50% stimulatory concentration [EC_{50}] values) from *in vitro* assays measuring cAMP response to SAR441255 and the endogenous ligands GLP-1(7-36)NH_2, GCG, and GIP(1-42) in HEK293 cells expressing human recombinant GLP-1R, GCGR, or GIPR (n = 4).

(D) Agonist potencies (EC_{50} values) in cell lines with endogenous expression levels of receptors assessing cAMP elevation (GLP-1R and GCGR) or lipolysis (GIPR) (n = 3–6).

are currently no approved pharmacological therapies. The physiological and pharmacological actions of the peptide hormones glucose-dependent insulinotropic peptide (GIP) and glucagon (GCG), including glucose-dependent insulin secretion, appetite suppression, energy expenditure, and hepatic fat oxidation, are likely to complement the beneficial effects of GLP-1 (Finan et al., 2016; Müller et al., 2017; Perry et al., 2020). Since the three endogenous peptide hormones GLP-1, GIP, and GCG share a high degree of sequence homology, it is feasible to generate analogs that activate each of the three receptors with similar activity as the individual endogenous ligands (Bhat et al., 2013a, 2013b; Gault et al., 2013). DiMarchi and colleagues in 2015 described such a highly potent unimolecular triagonist using carefully selected amino acids from the three native peptide hormones in combination with several stabilizing motifs (Finan et al., 2015). The resulting triagonist was evaluated in a series of preclinical rodent models of obesity and diabetes, showing impressive effects on body weight reduction and improved glucose control (Finan et al., 2015). Based on these highly promising preclinical data, several GLP-1-based unimolecular dual and triagonists have been subsequently evaluated (Clemmensen et al., 2019; Day et al., 2009; Di Prospero et al., 2021; Evers et al., 2020; Finan et al., 2013, 2015). To date, clinical data have only been published for dual incretin agonists (Ambery et al., 2018a; Di Prospero et al., 2021; Finan et al., 2013; Frias et al., 2017; Frías et al., 2021; Nahra et al., 2021; Portron et al., 2017; Rosenstock et al., 2021; Schmitt et al., 2017; Tillner et al., 2019). In this manuscript, we report preclinical and clinical data for a novel unimolecular GLP-1, GIP, and GCG receptor triagonist that offers potential for significant benefit in the treatment of metabolic diseases.

RESULTS AND DISCUSSION

SAR441255 structure and *in vitro* activity profile

The structure of SAR441255 is based on the selective GLP-1R agonist exendin-4. In exendin-4, the C-terminal sequence (residues 30–39) cages Trp25 (tryptophan cage), which provides enhanced helicity and structural stability to the peptide through intramolecular interactions and results in improved physicochemical and metabolic stability compared with the native peptides GLP-1, GCG, and GIP (Chabenne et al., 2010). Following careful analysis of 3D structural models based on the known X-ray structures of the three natural hormones in their respective receptors (Evers et al., 2018), amino acids (AAs) of GLP-1 at positions 17 and 21, of GCG at position 18, and of GIP at positions 19 and 28 were introduced to enhance receptor activation at the GCG and GIP receptors (Figure 1A). In position 2, an Aib (2-aminoisobutyric acid) was introduced to further strengthen activation of all three receptors as well as to protect against dipeptidyl peptidase IV (DPP-IV) cleavage, a major clearance pathway for GLP-1 and GIP (Deacon, 2004). Four AAs were mutated in the exendin tail (positions 32, 34, 35, and 39) to improve the physicochemical profile in the presence of antimicrobial preservatives, particularly to avoid aggregation issues at acidic pH in the presence of phenolic preservatives (Evers et al., 2019). Further AA changes at positions 3, 13, 20, and 29 were introduced to achieve high and balanced activation at each receptor and to ameliorate chemical stability in buffer formulations (Evers et al., 2020). While the combination of all 4 changes is needed to achieve the desired overall profile, Leu in position 13 was especially important to ensure chemical stability in solution and the other 3 AAs to achieve high GIPR activation. At position 14, a C16 fatty acid (palmitic acid) side chain was introduced at the

ϵ-amino group of lysine using two γ-glutamic acid spacers to prolong *in vivo* half-life via albumin binding (Bech et al., 2018). Figure 1B shows the resulting 3D model.

SAR441255 displayed high potency for stimulating human GLP-1, GCG, and GIP receptors expressed recombinantly in HEK293 cells, as assessed by monitoring cAMP accumulation. The peptide displayed potency (mean apparent 50% stimulatory concentration [EC_{50}] values of 1.03, 1.01, and 0.73 pM at GLP-1R, GCGR, and GIPR, respectively) (Figure 1C) and maximal activity (data not shown) that were comparable to those displayed by endogenous agonists for the cognate receptors (Figure 1C). Similarly, SAR441255 displayed high potency and maximal activity for stimulating mouse and monkey GLP-1, GCG, and GIP receptors expressed recombinantly in HEK293 cells (Table S1). We did not directly compare SAR441255 to mouse and rat GIP in these assays, which have been previously reported to show higher potency and maximal activation compared to human GIP (Mroz et al., 2019; Sparre-Ulrich et al., 2016).

To confirm these activities in a translational setting, the *in vitro* activity of SAR441255 was studied in cell systems expressing endogenous levels of each receptor. GLP-1R agonism was assessed using the human pancreatic cell line 1.1B4, with SAR441255 showing similar potency to endogenous ligand GLP-1 (EC_{50} values of 27 and 29 pM, respectively) (Figure 1D). GCGR agonism was tested in primary human hepatocytes using a buffer system containing 0.1% bovine serum albumin (BSA). SAR441255 exhibited comparable potency to endogenous GCG (EC_{50} values of 2.1 and 3.0 nM, respectively). GIPR agonism was studied by monitoring lipolysis in human adipocytes differentiated *in vitro* from precursors. Again, SAR441255 showed a similar potency as the endogenous ligand GIP (EC_{50} values of 42 and 102 pM, respectively). The maximal activity of SAR441255 at GLP-1, GCG, and GIP receptors was similar to the cognate endogenous agonist of each receptor. Overall, SAR441255 was shown to possess a balanced activity profile both in HEK293 cells that recombinantly overexpress the three receptors and in cell lines expressing endogenous receptor densities. The potencies closely approximate the potency of the cognate ligands for their respective receptors.

Metabolic effects of SAR441255 in a diet-induced obesity mouse model

Based on this promising *in vitro* profile, SAR441255 was characterized in a mouse model of diet-induced obesity (DIO) to study its effects on body weight. Twenty-five-week-old obese female C57BL/6NHsd mice (n = 8/group) were treated for 28 days with different subcutaneous (s.c.) doses of SAR441255 (0.3, 1, 3, 10, or 30 μg/kg) administered twice daily (bid). Based on the results of an earlier single-dose pharmacokinetic study in lean mice (mean half-life [$t_{1/2}$] = 5.9 h; data not shown), bid dosing was used to ensure sufficient SAR441255 exposure over a 24 h period. This decision was analogous to the bid dosing used for the GLP-1R agonist liraglutide in DIO mouse studies where a similar $t_{1/2}$ (4 h) ensured adequate coverage for GLP-1 receptor activation over 24 h (Elvert et al., 2018b; European Medicines Agency, 2009; Knudsen, 2010; Madsen et al., 2010; Raun et al., 2007; Tølbøl et al., 2018).

Three comparator groups were studied: a group of chow-fed lean mice treated with vehicle and two groups of DIO mice, one treated with vehicle and the other with a previously identified mouse GLP-1R/GCGR dual agonist (30 μg/kg s.c. bid) (Elvert et al., 2018b). Dose-dependent effects on body weight change were observed following treatment with SAR441255. Compared with baseline, the obese vehicle-treated control group exhibited a body weight change of +11.5% on day 26 (Figure 2A). Body weight changes on day 26 with increasing doses of SAR441255 (0.3, 1, 3, 10, and 30 μg/kg bid) were +9.7%, +6.9%, +5.8%, −4.8%, and −14.1%, respectively. SAR441255 doses of 3 μg/kg or greater showed statistically significant reductions in body weight compared with vehicle-treated obese controls (Figure 2B). Due to a forced fasting period prior to a dual energy X-ray absorptiometry (DEXA) scan on day 26, further body weight changes were not analyzed. Cage side observations were routinely made following administration of SAR441255. No gross changes in behavior were noted at the administered doses. Other researchers have similarly reported a lack of significant behavioral effects with administration of GLP-1 analogs or triagonists to rodents at appropriate dose levels (Finan et al., 2015; Talsania et al., 2005). Hence, the effect on body weight change is not due to altered feeding behavior but likely results from the satiety effects and increased energy expenditure attributed to activation of GLP-1R and GCGR, respectively (Kleinert et al., 2019; Müller et al., 2019).

Nonfasted blood glucose levels were significantly lower for SAR441255-treated mice at doses of 1 μg/kg or greater as compared with vehicle-treated obese controls (Table S2). A dose-dependent reduction in liver weight was observed on day 28, with the 10 and 30 μg/kg SAR441255 groups being significantly lower than the vehicle control group ($p < 0.001$ and $p < 0.0001$, respectively) (Table S3). In addition, dose-dependent decreases in serum AST and ALT levels were observed, indicative of improved liver function in the SAR441255-treated mice. Compared with obese control mice, mean serum ALT levels were reduced by 73% and 81% for the SAR441255 10 and 30 μg/kg bid groups ($p < 0.001$ and $p < 0.0001$, respectively). Similarly, mean AST levels were reduced by 46%, 55%, and 58% in the SAR441255 3, 10, and 30 μg/kg bid groups versus obese controls ($p < 0.001$, $p < 0.0001$, and $p < 0.0001$, respectively). These observations are consistent with results previously reported by Finan and colleagues using a different balanced triagonist of GLP-1, GIP, and GCG receptors (Finan et al., 2015). The 30 μg/kg bid dose of SAR441255 also showed a significantly greater reduction in body weight (14.1%) compared with the mouse GLP-1R/GCGR dual agonist comparator (6.3%) administered at the same dose. The dual agonist produced a similar reduction in liver weight (−35%) and a decrease in mean serum ALT (−72%) and AST (−51%) levels versus obese controls (Table S3).

As mouse metabolism, especially feeding behavior, basal metabolic rate, and primary site of glucose disposal, differs from human metabolism (Kleinert et al., 2018; Vaughan and Mattison, 2016), further investigation to study the interplay of activation of all three receptors was undertaken using obese diabetic cynomolgus monkeys, a more relevant translational preclinical model.

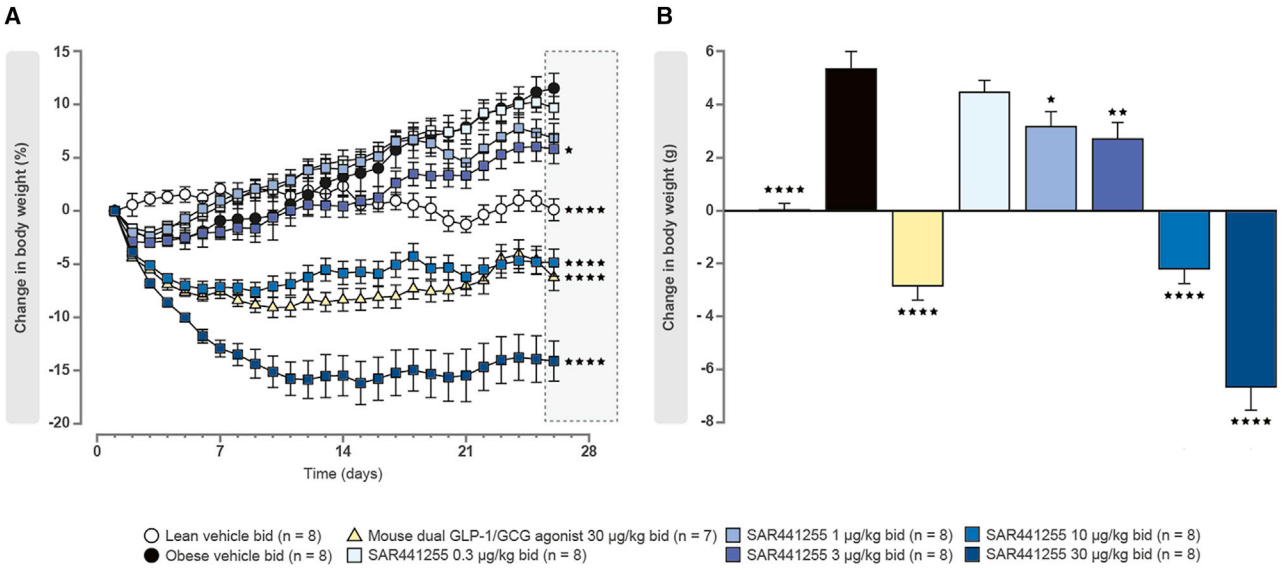

Figure 2. Effect of SAR441255 on body weight in diet-induced obese (DIO) C57BL/6NHsd mice

Relative (A) and absolute (B) change following twice-daily treatment (26 days) with vehicle, mouse dual GLP-1R/GCGR agonist (30 µg/kg), or increasing doses of SAR441255.

Values represent means ± SEM. Baseline values (just before first dosing on day +1) were compared with results at study end (day +26). Dose-dependent treatment effects versus obese vehicle control group were analyzed with one-way ANOVA at study end (day +26) followed by Dunnett's test for pairwise comparisons between each treated and obese control group. *p < 0.05, **p < 0.01, ****p < 0.0001 versus obese vehicle control.

SAR441255 treatment ameliorates body weight and metabolic parameters in obese diabetic cynomolgus monkeys

DIO and diabetic cynomolgus monkeys (*Macaca fascicularis*) were treated with SAR441255, another triple GLP-1/GIP/GCG agonist peptide 12 (Evers et al., 2020), a monkey dual GLP-1/GCGR agonist (Elvert et al., 2018b), or vehicle for 42 days. Comparative *in vitro* data for SAR441255, peptide 12, and the dual agonist on monkey receptors are shown in Table S1. Doses were increased in four steps every 3 days—3, 5, 8, and 11 µg/kg for SAR441255; 3, 5, 8, and 10 µg/kg for peptide 12; and 1, 2, 3, and 4 µg/kg for the dual agonist—reaching the maintenance dose on day 10. Doses were selected to achieve similar plasma exposure (area under the curve [AUC]) based on the results of a prior pharmacokinetics study in lean cynomolgus monkeys (data not shown). Top-line body weight and HbA1c data for peptide 12 have been previously reported (Evers et al., 2020) and are not included in this report. Vehicle and dual agonist comparator data included in this previous report are described here in greater detail. Body weight and glycated hemoglobin (HbA1c) levels remained stable in vehicle-treated monkeys throughout the study. In comparison, a significant reduction in body weight was observed following SAR441255 (−12.6% ± 1.74%, $p < 0.05$) or dual agonist (−8.1% ± 1.7%, $p < 0.05$) (Evers et al., 2020) treatment (Figures 3A and 3B). Similarly, HbA1c values were significantly decreased following treatment with SAR441255 (−1.37% ± 0.34%, $p < 0.05$) and the dual agonist (−1.85% ± 0.37%, $p < 0.05$) (Evers et al., 2020) (Figure 3C). In both treatments, HbA1c values below 5% were achieved at study end, a level consistent with normoglycemia in this species (Marigliano et al., 2011). In addition, fasting plasma glucose (FPG) and ALT levels were significantly lowered with SAR441255, but not with the dual agonist, with various lipid parameters showing a non-significant reduction in both treatment groups (Table S4).

Total ketones, 3-hydroxybutyrate, and fibroblast growth factor 21 (FGF21) levels are three biomarkers that have previously been used to assess GCGR action (Müller et al., 2017). These parameters were measured to determine whether they were suitable biomarkers to document GCG receptor activation in the context of triple GLP-1R/GCGR/GIPR agonism with SAR441255. In all groups, total ketones and 3-hydroxybutyrate levels at baseline were <150 µmol/L (Figures 3D and 3E). Following treatment for 6 weeks, total ketones and 3-hydroxybutyrate levels in the vehicle and monkey dual agonist treatment groups remained relatively unchanged, a finding consistent with previous observations (Elvert et al., 2018b). In contrast, a trend toward higher values was observed in the SAR441255 11 µg/kg dose group at the end of the study. FGF21 levels in the vehicle group were unchanged at study end while showing a non-significant increase in the dual- and triagonist-treated groups (Figure 3F). These findings indicate that total ketones, 3-hydroxybutyrate, and FGF21 levels were not reliable biomarkers to assess GCGR activation in the context of concomitant GLP-1R and GIPR activation. Taken together, the study findings suggest that biomarkers that are independent of GLP-1R and GIPR activation are required to unambiguously demonstrate GCGR engagement.

Regarding dual GLP-1R/GCGR agonism, we recently reported that co-administration of a selective GLP-1R agonist with a selective GCGR agonist in obese diabetic monkeys led to greater weight loss compared to treatment with each of the individual components (Elvert et al., 2018a). However, we also noted glycemic control was worse in the group co-administered agonists of both GLP-1R and GCGR compared to the group treated with an

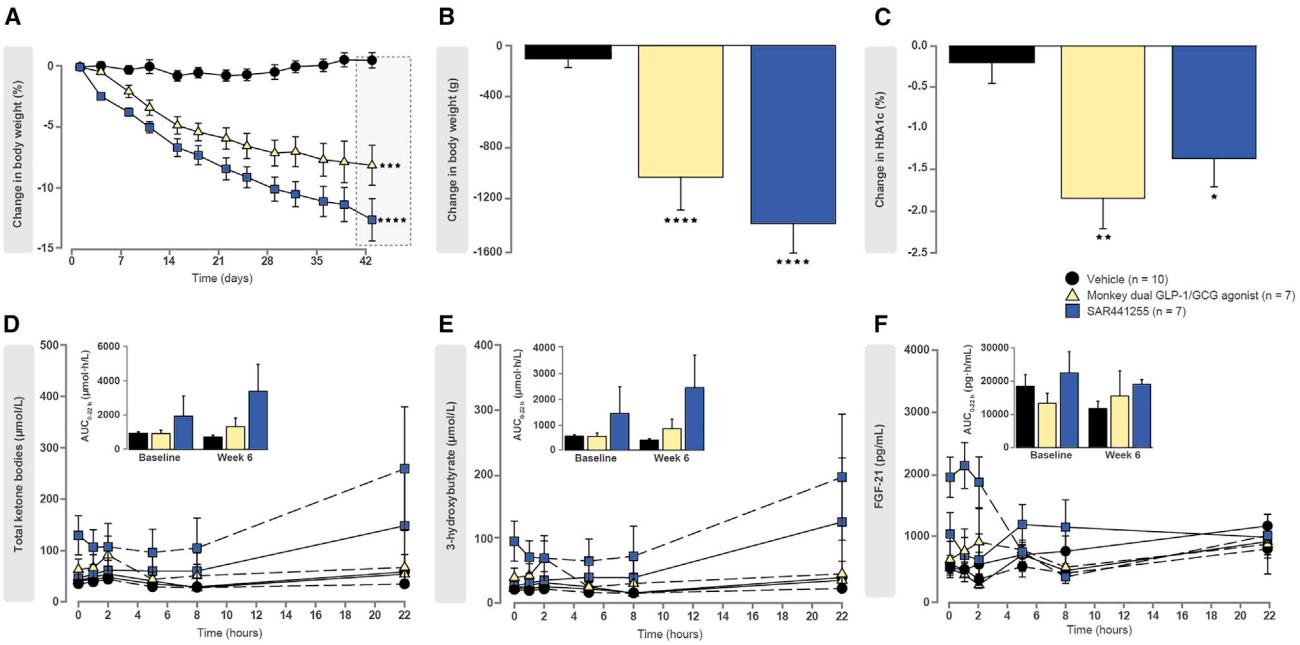

Figure 3. SAR441255 ameliorated body weight and improved glycemic control in obese diabetic cynomolgus monkeys

(A–C) Relative (A) and absolute (B) change in body weight and change in HbA1c levels (%) (C) in obese diabetic cynomolgus monkeys following treatment with vehicle (n = 10), monkey dual GLP-1R/GCGR agonist (4 μg/kg) (n = 7), or 11 μg/kg SAR441255 (n = 7). The baseline values for body weight (A and B) on day 1 and for HbA1c (%) (C) on day −21 were compared to values at study end (days +42/43). Change in body weight and HbA1c data for vehicle and monkey dual GLP-1R/GCGR agonist were shown in Evers et al. (2020).

(D–F) Time course of change in plasma total ketone bodies (D), 3-hydroxybutyrate (E), and fibroblast growth factor 21 (FGF-21) (F) levels over 22 h following treatment with vehicle, monkey dual GLP-1R/GCGR agonist (4 μg/kg), or 11 μg/kg SAR441255. Values at baseline (pre-treatment, day −6) are shown as solid lines and after 6 weeks (days 42/43) are shown as dashed lines. Area under plasma-concentration-time curve from time zero to 22 h ($AUC_{0\text{-}22\ h}$) for each parameter is shown in the respective insets.

Values represent means ± SEM. Differences were determined using one-way ANOVA followed by Dunnett's test to compare treatment effects versus vehicle control group. $p < 0.05$ was considered statistically significant. *$p < 0.05$, **$p < 0.01$, ***$p < 0.001$, ****$p < 0.0001$ versus vehicle control group.

agonist of the GLP-1R alone. Similar findings were previously reported in DIO rodents (Day et al., 2012).

Compared with these earlier findings, treatment with the triagonist SAR441255 resulted in substantial weight loss in obese diabetic monkeys without impairing glucose control. Compared to the dual GLP-1R/GCGR agonist, triple agonist SAR441255 shows considerably greater potency at the GCG receptor (EC_{50} of 6.6 versus 119.3 pM) (Table S1) (Elvert et al., 2018b). This substantial increase in GCGR activity in combination with the effects of GIP pharmacology are expected to provide additional improvement in body weight reduction compared with dual GLP-1/GCG receptor agonism (Mroz et al., 2019; Samms et al., 2020; Zhang et al., 2021). Importantly, this increase in GCGR activity with SAR441255 did not lead to a significant deterioration in glycemic control. The strong additional GIPR agonist component of SAR441255 in combination with the GLP-1R agonist component counterbalanced the hyperglycemic effects typically elicited by activating the GCG receptor component. The importance of the second glucose-lowering GIP component is underlined by a recent report of a dual GLP-1R/GCGR agonist (JNJ-64565111) with high potency at the GCG receptor. Among individuals with T2D and obesity, a significant dose-dependent reduction in body weight was observed without any improvement in glycemic control (no HbA1c reduction, increased FPG) (Di Prospero et al., 2021).

Our collective observations in obese diabetic monkeys (Elvert et al., 2018a, 2018b; Evers et al., 2020) support previous observations in obese rodents (Finan et al., 2015) that suggest GCG and GIP on top of GLP-1R pharmacology provide additional benefit for body weight reduction in these translational obesity models.

SAR441255 exhibited GLP-1 and GCG receptor occupancy in a PET study in lean cynomolgus monkeys

While the contributions of GLP-1, GIP, and GCG receptor activation by triagonist peptides to the overall pharmacology can be deduced from *in vivo* studies that compare pharmacological effects elicited by triagonist peptides to monoagonists or dual agonist peptides, performing combination studies or investigations in single and double knockout rodents, it is difficult to predict the level of engagement elicited at each receptor. Further, available circulating biomarkers to detect receptor engagement have not been clinically validated and do not provide (semi)quantitative estimates. To further understand engagement of the different receptors *in vivo*, receptor occupancy of SAR441255 at the GLP-1 and the GCG receptors was studied with the use of positron emission tomography (PET) imaging following radiotracer administration in lean cynomolgus monkeys. Single s.c. doses of 11 μg/kg SAR411255, the maintenance dose used in the

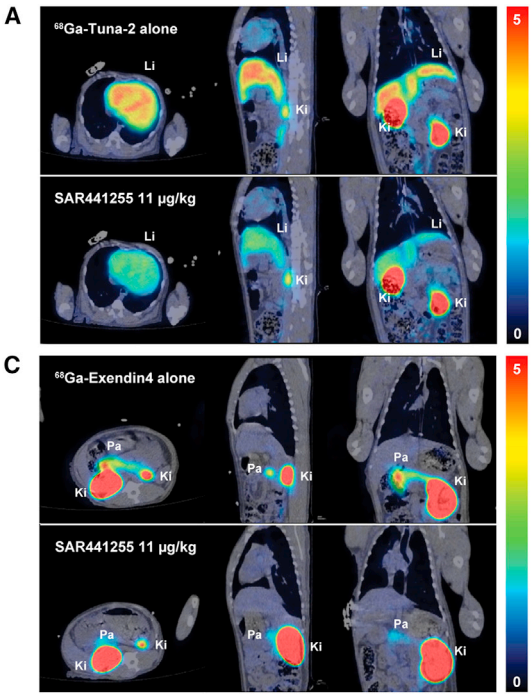

Figure 4. SAR441255 showed high GLP-1 and GCG receptor occupancy in a PET study in lean cynomolgus monkeys

Receptor occupancy of GCGR and GLP-1R in lean monkeys following administration of SAR441255 (11 μg/kg, s.c.). Representative standardized uptake value (SUV) images of GCGR (A) and GLP-1R (C) occupancy examinations are shown at baseline (top panels) and after treatment with SAR441255 (bottom panels). SUV values between 0 and 5 are shown in scale on the right of each figure (A and C). Decrease in the binding of each radiotracer (as measured by V_t) in respective tissue is indicative of specific receptor binding by SAR441255 (B and D). Li, liver; Pa, pancreas; Ki, kidney.

obese diabetic monkey study, were administered together with radiotracers. We used an exendin-4-based GLP-1R radiotracer [^{68}Ga]Ga-DO3A-Exendin-4 (Selvaraju et al., 2013) and a newly developed GCGR tracer [^{68}Ga]Ga-DO3A-Tuna-2 (Eriksson et al., 2020; Eriksson et al., 2019; Velikyan et al., 2019) to assess engagement of GLP-1R in the pancreas and GCGR in the liver, respectively. Unfortunately, the lack of a suitable radiotracer (at the time of conducting this study) with sufficient potency to assess GIP receptor occupancy precluded investigation of target engagement at this receptor by SAR411255.

Each tracer was administered intravenously on a separate day to monkeys and a baseline PET scan was performed (Table S5). Strong signals from the target organs (liver and pancreas for [^{68}Ga]Ga-DO3A-Tuna-2 and [^{68}Ga]Ga-DO3A-Exendin-4, respectively) and the kidneys, the latter being the predominant mode of excretion, were observed (Figures 4A and 4C). Following signal disappearance, monkeys were treated with 11 μg/kg SAR441255 s.c., and 2 h later, when exposure of SAR441255 approached the maximum concentration (C_{max}), a second tracer dose was administered, and a second PET scan was performed. Mean decreases in signal intensity from baseline for liver (reflecting GCGR occupancy) and the pancreas (reflecting GLP-1R occupancy) were 40.6% and 72.5%, respectively (Figures 4B and 4D). This strong decrease in signal from the target organs in the repeat PET scan indicated that a significant number of the receptors in the target organs were occupied by SAR441255 and were therefore not available for tracer binding. Previous studies with the GCG tracer [^{68}Ga]Ga-DO3A-Tuna-2 (doses up to 67 μg/kg) show that treatment with a highly potent acylated selective GCGR agonist (30 μg/kg) results in signal reductions (and thereby receptor occupancy) in the liver of up to 70% (Eriksson et al., 2019). Similarly, high doses of the unlabeled GLP-1R tracer [^{68}Ga]Ga-DO3A-Exendin-4 (20 μg/kg) have shown signal reductions of up to 100% in the pancreas (Selvaraju et al., 2013), reflecting complete GLP-1R occupancy. The high target engagement of GCGR and GLP-1R with the 11 μg/kg dose of SAR441255 administered to lean monkeys in this study was consistent with the findings observed in obese diabetic monkeys where the same dose demonstrated a robust reduction in body weight and improved glycemic control.

Cardiovascular safety of SAR441255 in lean telemetered cynomolgus monkeys

Conscious freely moving cynomolgus monkeys (*Macaca fascicularis*) were treated with once-daily s.c. doses of SAR441255 (3, 30, or 300 μg/kg) or vehicle for 4 days. Heart rate (beats per min) and systolic blood pressure (SBP) measurements were continuously recorded every 15 min on day 1 over 24 h post-dose and on day 4 over 48 h post-dose via an implanted telemetry unit. A dose-related increase in heart rate lasting up to 10–11 h was observed following administration of the low (3 μg/kg) and mid (30 μg/kg) doses of SAR441255 on day 1; this lasted for up to 20 h in the highest (300 μg/kg) SAR441255 dose group (Figure S1). The initial increase in heart rate fully disappeared by day 4 in the low and mid SAR441255 doses but remained slightly above that of the vehicle-treated group in the high 300 μg/kg dose group and fully disappeared by day 5. There were no statistically significant dose-related changes in SBP on day 1 following SAR441255 administration (Figure S2). On day 4, when compared to vehicle control, all doses of SAR441255 induced a statistically significant decrease in SBP. The decrease in SBP was slight (<10 mmHg) and lasted over 24 h. By day 5, SBP values in the 30 and 300 μg/kg/day groups remained significantly below those of the vehicle control group.

Based on the preclinical data demonstrating that SAR441255 is a potent unimolecular triagonist that activates all three receptors *in vitro*, provides better weight loss compared with unimolecular dual GLP-1/GCG receptor agonists in mice and monkey models, and does not show any major adverse cardiovascular effects in lean monkeys, SAR441255 was advanced into clinical testing.

Phase 1 study with SAR441255 in lean to overweight healthy subjects

A randomized, double-blind, single-center, placebo-controlled trial assessed the safety, tolerability, pharmacokinetics, and pharmacodynamics of single ascending s.c. doses of SAR441255 in lean to overweight healthy subjects (registered on ClinicalTrials.gov as NCT04521738). Forty-eight healthy subjects were randomized to SAR441255 (3, 9, 20, 40, 80, or 150 μg) or placebo in a 3:1 ratio. All participants completed the study. The baseline characteristics are described in Table S6.

Non-compartmental pharmacokinetic parameters for SAR441255 in plasma estimated after single doses of 20, 40, 80, and 150 μg are summarized in Table S7. Most subjects enrolled in the 3 and 9 μg dose groups had insufficient quantifiable SAR441255 concentrations for pharmacokinetic parameters to be reported. The plasma concentration-time profile of the 20 to 150 μg doses of SAR441255 is shown in Figure S3. Increasing doses were associated with higher plasma concentrations and overall exposure.

Following s.c. administration, SAR441255 absorption was steady, with the median C_{max} reached by 3.0 to 3.5 h. After reaching C_{max}, SAR441255 was eliminated in a monophasic manner, with a mean elimination terminal half-life of 3.5 to 6.1 h across the 20 to 150 μg range (Table S7). SAR441255 exposure (mean C_{max} and AUC) following single s.c. doses showed an approximate dose-proportional increase across the 20 to 150 μg range. CL/F was also relatively stable across the 20 to 150 μg dose range. Collectively, the data were consistent with linear pharmacokinetics across the 20 to 150 μg dose range.

Plasma glucose, insulin, and C-peptide profiles following administration of SAR441255 were determined before and after a mixed-meal test (MMT). Data for the clinically relevant SAR441255 doses of 80 and 150 μg are presented here in greater detail.

Following administration of single doses of SAR441255 in the fasting state, maximal reduction in blood glucose levels were observed at 1 h post-dose, a finding consistent with GLP-1R agonism (Owens et al., 2013). At this time point, 3 of 6 subjects who received the 80 μg dose and all 6 subjects who received the 150 μg dose with normal glucose values at baseline had glucose levels that were less than 3.9 mmol/L, a threshold generally used to define hypoglycemia (International Hypoglycaemia Study Group, 2015). None of the subjects reported clinical signs or symptoms of hypoglycemia. The corresponding mean plasma glucose levels in the two dose groups across all subjects at 1 h post-dose were 3.75 and 3.52 mmol/L, respectively (Figure 5A). Further low blood glucose values (i.e., $\leq$3.9 mmol/L) were not observed in either dose group at subsequent time points on day 1 or in the placebo cohort. Blood glucose levels subsequently returned to baseline levels within 1 to 2 h. In contrast, fasting insulin and C-peptide levels remained relatively stable and showed no correlation with the glucose levels (Figures 5B and 5C).

The reason for this relatively prompt and consistent reduction in blood glucose levels is at present unexplained. The low blood glucose values at ~1 h post-dose occurred earlier than the C_{max} of ~3 h following SAR441255 administration (Table S7). The rapid recovery to baseline levels within 1 to 2 h is thought to be a result of the pharmacological activities of GCG and GIP within the triple agonist that helps to balance the incretin effects. GCG is a well-known counter-regulatory hormone to insulin. Recent data also establish that GIP, in contrast to GLP-1, promotes release of GCG in conditions of hypoglycemia (Ahrén et al., 2009; Christensen et al., 2011, 2014). This counter-regulatory effect of GIP has also been observed in healthy subjects and in people with T2D (Christensen et al., 2014). Further evaluation will be required to assess if this phenomenon is particular to SAR441255 or is observed with other triagonists, and whether it occurs with multiple dosing or is limited to the first dose.

Following the MMT, a dose-dependent reduction in postprandial plasma glucose (PPG), insulin, and C-peptide levels was observed with the 80 and 150 μg doses of SAR441255 compared with a slight increase in the placebo group (Figures 5A–5C). All participants fully consumed and tolerated the offered MMT. The reduction in postprandial insulin and C-peptide levels suggests that the effect on PPG reduction is driven by inhibition of gastric emptying, a mechanism consistent with the effect observed with selective GLP-1 receptor engagement (Marathe et al., 2013; Owens et al., 2013). Näslund and colleagues showed that an infusion of GLP-1(7-36)NH_2 given in conjunction with a solid mixed meal delayed scintigraphic solid gastric emptying in healthy male subjects (Näslund et al., 1999). After 180 min, there was 65% of the food remaining in the stomach compared with less than 10% in the saline-treated comparator group. This resulted in a reduced increase in plasma glucose concentrations in parallel with reduced insulin and C-peptide levels. Similar effects have been described with the short-acting GLP-1R agonist lixisenatide, where glucose levels were reduced with a delayed increase in C-peptide levels (Becker et al., 2015; Lorenz et al., 2013).

Since gastric emptying effects with long-acting GLP-1 agonists attenuate over time (Umapathysivam et al., 2014; Urva et al., 2020), we believe this phenomenon will not play a significant role in long-term glucose control, and the insulinotropic character of the three involved principles will become the major driving force for glucose control.

Single doses of SAR441255 up to 150 μg were well tolerated. Gastrointestinal disorders (nausea, vomiting, dry mouth, and mouth ulceration) were the most frequent treatment-emergent adverse events (TEAEs) reported following treatment with SAR441255 (Table 1). Nausea was the most frequent TEAE in the highest 150 μg dose group with 3 events (3 of 6 subjects) reported. All events were mild in severity, occurred between 3 and 4 h after SAR441255 treatment, and were assessed as related to SAR441255 treatment. One subject in the 150 μg dose group reported a single episode of vomiting (the subject also reported nausea), but this was assessed as not being related to SAR441255 treatment. The frequency of gastrointestinal TEAEs, specifically nausea and vomiting, was consistent with that reported in other healthy volunteer studies evaluating selective GLP-1RAs and dual receptor agonists (Ambery et al., 2018b; Coskun et al., 2018; Tillner et al., 2019). TEAEs were reported in 3 of 12 subjects (25.0%) who received placebo and in 10 of 36 subjects (27.8%) who received SAR441255. The incidence of TEAEs was the highest in the 80 and 150 μg dose groups. In the remaining dose groups (3, 9, and 20 μg), the incidence of TEAEs was similar to placebo. No serious TEAEs, TEAEs leading to permanent discontinuation, or severe TEAEs were reported during the study. Except for one AE of lipase increased rated as being of moderate intensity, all TEAEs were graded as mild

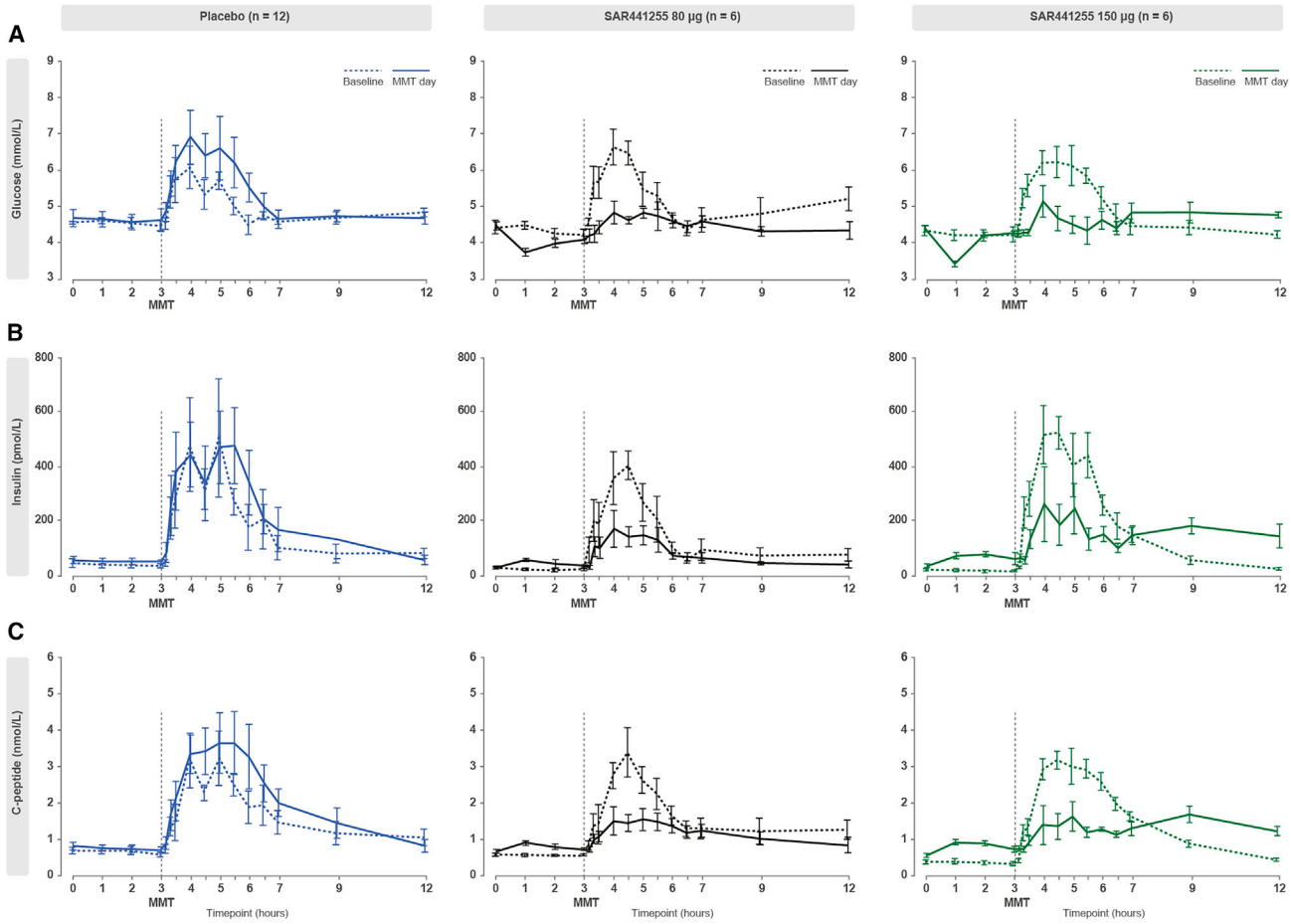

Figure 5. SAR441255 showed a dose-dependent reduction in PPG, insulin, and C-peptide levels in humans

Glucose (A), insulin (B), and C-peptide (C) profiles following a mixed-meal test (MMT). Baseline (day −1, dashed line) and MMT day profiles (day 1, solid line) are shown for placebo (blue color, n = 12), 80 µg SAR441255 (black color, n = 6), and 150 µg SAR41255 (green color, n = 6). The vertical dotted line indicates the time of MMT dosing. Values represent means ± SEM.

in severity and mainly comprised the limiting gastrointestinal disorders. No hypersensitivity reactions were reported during the study.

Despite no dose-limiting TEAEs, dose escalation was stopped at the 150 µg dose. This was unrelated to the safety and tolerability of SAR441255 but linked to changes in company strategy.

Besides the expected changes in plasma glucose, there was no evidence of treatment- or dose-related trends in any of the laboratory parameters measured. No significant changes in blood pressure were noted, and electrocardiogram (ECG) analysis showed no changes in the QTc interval in any of the treatment groups. At the 150 µg SAR441255 dose level, heart rate (from standard 12-lead ECGs) was higher compared to the other dose groups on the treatment day (day 1) and tended to increase above that observed in the placebo group (Figure S4A). No difference was observed in subsequent days up to the last study visit on day 8. Heart rate data extracted from the 24 h continuous Holter ECG monitoring also showed a trend toward an increase in heart rate in the 150 µg dose group compared with placebo over the whole observation period (Figure S4B). These results were consistent with an initial dose-dependent increase in heart rate observed in conscious, telemetered lean cynomolgus monkeys when increasing doses of SAR441255 (3, 30, or 300 µg/kg) were administered once daily for 4 days (Figure S1). In addition, repeated doses of SAR441255 in this same study induced a statistically significant decrease in SBP compared with vehicle control on day 4 (Figure S2). While no effect on blood pressure was observed in our single-dose healthy volunteer study, increases in heart rate and a reduction in blood pressure are well-characterized effects of GLP-1 receptor agonist activity (Heuvelman et al., 2020; Lorenz et al., 2017) and have been observed in larger studies with the dual GIP/GLP-1R agonist tirzepatide (Frías et al., 2021; Rosenstock et al., 2021). The effects of GCGR agonism on hemodynamic parameters are at present not clearly defined (Petersen et al., 2018). None of the subjects developed anti-SAR441255 antibodies during the study.

Effects of SAR441255 on C-telopeptide of cross-linked type I collagen and AAs

For chimeric peptides exerting effects on multiple receptors with overlapping downstream effects, it is important to discriminate between the contribution of individual agonistic component

Table 1. Treatment-emergent adverse events for placebo and SAR441255 groups by primary system organ class and preferred term (safety population)

Primary system organ class preferred term, n (%)	Placebo (N = 12)	SAR441255 dose					
		3 μg (N = 6)	9 μg (N = 6)	20 μg (N = 6)	40 μg (N = 6)	80 μg (N = 6)	150 μg (N = 6)
Any TEAE class	3 (25.0)	1 (16.7)	2 (33.3)	1 (16.7)	0	3 (50.0)	3 (50.0)
Nervous system disorders							
Dizziness	0	0	0	0	0	1 (16.7)	1 (16.7)
Dizziness postural	1 (8.3)	0	1 (16.7)	0	0	0	0
Headache	2 (16.7)	0	0	0	0	0	0
Gastrointestinal disorders							
Nausea	0	0	0	0	0	0	3 (50.0)
Vomiting	0	0	0	0	0	0	1 (16.7)
Dry mouth	0	0	0	0	0	2 (33.3)	0
Mouth ulceration	1 (8.3)	1 (16.7)	1 (16.7)	0	0	0	0
Skin and subcutaneous tissue disorders							
Dry skin	0	0	1 (16.7)	0	0	0	0
Musculoskeletal and connective tissue disorders							
Arthralgia	0	0	0	1 (16.7)	0	0	0
General disorders and administration site conditions							
Catheter site extravasation	1 (8.3)	0	0	0	0	0	0
Fatigue	0	0	0	0	0	1 (16.7)	0
Injection site pain	0	0	0	0	0	1 (16.7)	0
Investigations							
ALT increased	0	0	1 (16.7)	0	0	0	0
Lipase increased	0	1 (16.7)	0	0	0	0	0
Orthostatic heart rate response increased	0	1 (16.7)	0	0	0	0	0
Injury, poisoning, and procedural complications							
Arthropod bite	1 (8.3)	0	0	0	0	0	0

N, total number of subjects treated within each group; n (%), number and % of subjects with at least one TEAE in each category. An AE is considered as treatment emergent if it occurred from the time of the first investigational medicinal product administration up to the end of study visit (included). AE, adverse event; ALT, alanine transaminase; TEAE, treatment-emergent adverse event. AEs were coded using MedDRA Version 22.0.

effects to the overall biological effect. Single-dose studies in humans are generally not sufficient to understand the complete pharmacological profile of compounds like SAR441255. To guide future chronic dosing studies, we were interested in a qualitative assessment of whether the receptor engagement observed in preclinical studies was translatable to humans. In this respect, the changes in PPG without any substantial increase in insulin levels following SAR441255 administration were consistent with previously described effects driven by the GLP-1R engagement (Drucker, 2018). To further delineate the target engagement of the GIP and GCG receptors by SAR441255, we used specific biomarkers for each receptor.

For the assessment of GIPR activation, C-telopeptide of cross-linked type I collagen (CTX), a marker of bone turnover (Ding et al., 2008) and a biomarker for GIPR engagement (Christensen et al., 2018; Gasbjerg et al., 2021; Nissen et al., 2014), was evaluated at multiple time points in the 80 and 150 μg dose groups. Baseline CTX values were comparable between placebo and these doses of SAR441255. Following SAR441255 administration, fasting CTX levels declined by more than 50% from baseline, showing a further postprandial decrease (after the MMT) in both dose groups (Figure 6A). In contrast, CTX levels in the placebo group remained relatively unchanged in the fasting state and only showed a decrease following the MMT. The observed decrease in CTX levels seen following SAR441255 administration suggests the potential utility of the component GIPR activity in improving bone health (Christensen et al., 2020) and merits further investigation. This is of particular interest as patients with T2D are at an increased risk of bone fractures despite having normal or increased bone density (Romero-Díaz et al., 2021).

In context of the observed CTX findings, several studies have evaluated the effects of GIP and GLP-1 administration on CTX levels. In one study, intravenous (i.v.) infusions of GIP decreased CTX levels in people with type 1 diabetes (T1D) under conditions of low and high plasma glucose (Christensen et al., 2018). A further study showed that oral administration of glucose (via an oral glucose tolerance test) induced a greater reduction in CTX levels compared with an isoglycemic i.v. glucose infusion designed to closely mimic the oral glucose load (Westberg-Rasmussen et al., 2017). This suggested that the differential effect on CTX response between the oral and i.v. infusion of glucose was predominantly influenced by gastrointestinal hormones, especially GIP, rather than glucose levels. A correlation was observed between the decline in CTX and peak GIP levels, while no association was detected with GLP-1, GLP-2, or insulin. However, other studies argue that GLP-1 infusions influence CTX plasma levels, which are dependent on the glycemic state. While an i.v. infusion of GLP-1 under conditions of high glycemia to overweight or obese men effectively lowered CTX levels (Bergmann et al., 2019), infusions of GLP-1 under conditions of low glucose to people with T1D has been shown to not lead to such a decrease (Christensen et al., 2018). Nissen and colleagues reported that injection of high-dose active GLP-1, GLP-1(7-36) amide, to healthy young individuals resulted in a prompt increase in plasma concentrations (C_{max} after 15 min) and a prompt but slight decrease in CTX levels, which were 25% lower after 2 h (Nissen et al., 2019). They also showed that administration of exendin-4 led to a slower increase in plasma levels (C_{max} 90 min) and a much slower decrease in CTX levels, which were 20% lower 2 h after injection.

Considering these more recent observations, a modest decrease of CTX levels via GLP-1R activation cannot be excluded. Our study, however, showed a substantial decrease in CTX levels of greater than 50% after 3 h following SAR441255 administration under conditions of low glucose prior to the MTT (Figure 6A). Substantial decreases in CTX were already observed after 1 h following dosing. These findings suggest that the observed lowering of CTX levels provides strong evidence for GIP receptor target engagement by SAR441255.

The GCGR-specific effects on the plasma levels of AAs have been well described (Boden et al., 1984; Kraft et al., 2017; Mu et al., 2012; Okamoto et al., 2015, 2017; Solloway et al., 2015). Recently, it has also been shown that AAs are sensitive and translatable GCGR-specific biomarkers for GLP-1R/GCGR dual agonists (Li et al., 2020). To test for GCGR-target engagement with SAR441255, we measured plasma levels of AAs over 12 h in the 80 and 150 μg dose cohorts. Baseline (day –1) AA profiles were similar for the placebo and 80 and 150 μg SAR441255 cohorts (Figure 6B). Following treatment, a substantial decrease in plasma AA levels over the following 3 h was observed in the 80 and 150 μg cohorts (shown in blue on heatmap) compared with baseline, indicating strong activation of hepatocytic GCGR pathways (Figure 6B). Further, the strong postprandial increase in plasma AA concentrations observed at baseline was attenuated in both SAR441255 groups (Figure 6C). Further, GLP-1R-mediated effects on gastric emptying may add to the direct effects mediated by the activation of the GCGR.

Using AAs as a specific biomarker of GCGR activation in this acute setting, we confirmed that the high target engagement of GCGR with SAR441255 observed in the monkey PET tracer study was translatable to humans. Further evaluation with multiple dosing of SAR441255 will be required to assess how these effects translate in a chronic setting. In particular, the GLP-1R-mediated delay in gastric emptying observed during the first weeks following initiation of GLP-1R therapy is likely to diminish due to tachyphylaxis following constant exposure to the triple agonist (Maselli and Camilleri, 2021; Nauck et al., 2011; Umapathysivam et al., 2014). Close monitoring of AA levels in long-term studies will also be crucial as levels of non-essential and essential AAs (e.g., leucine or tryptophan; Figure 6C) are likely to be impacted. In this regard, chronic AA deficiency should be avoided as it is linked to a plethora of diseases (Aliu et al., 2018). However, the mechanism by which elevated insulin secretion produced by GLP-1 and GIP receptor activity in triagonists counterbalances this AA effect remains unclear (Everman et al., 2016). Longer term studies with dual and triagonist molecules containing GCGR agonist activity will help to shed further light on this issue.

Final summary and implications

The results reported here show that SAR441255 is a highly potent triagonist targeting GLP-1, GCG, and GIP receptors with balanced activation of all three targeted receptors. Following chronic treatment, enhanced effects on each of the metabolic outcomes, superior to those achieved with a dual GLP-1/GCG receptor agonist (Elvert et al., 2018b), were

CellPress
OPEN ACCESS

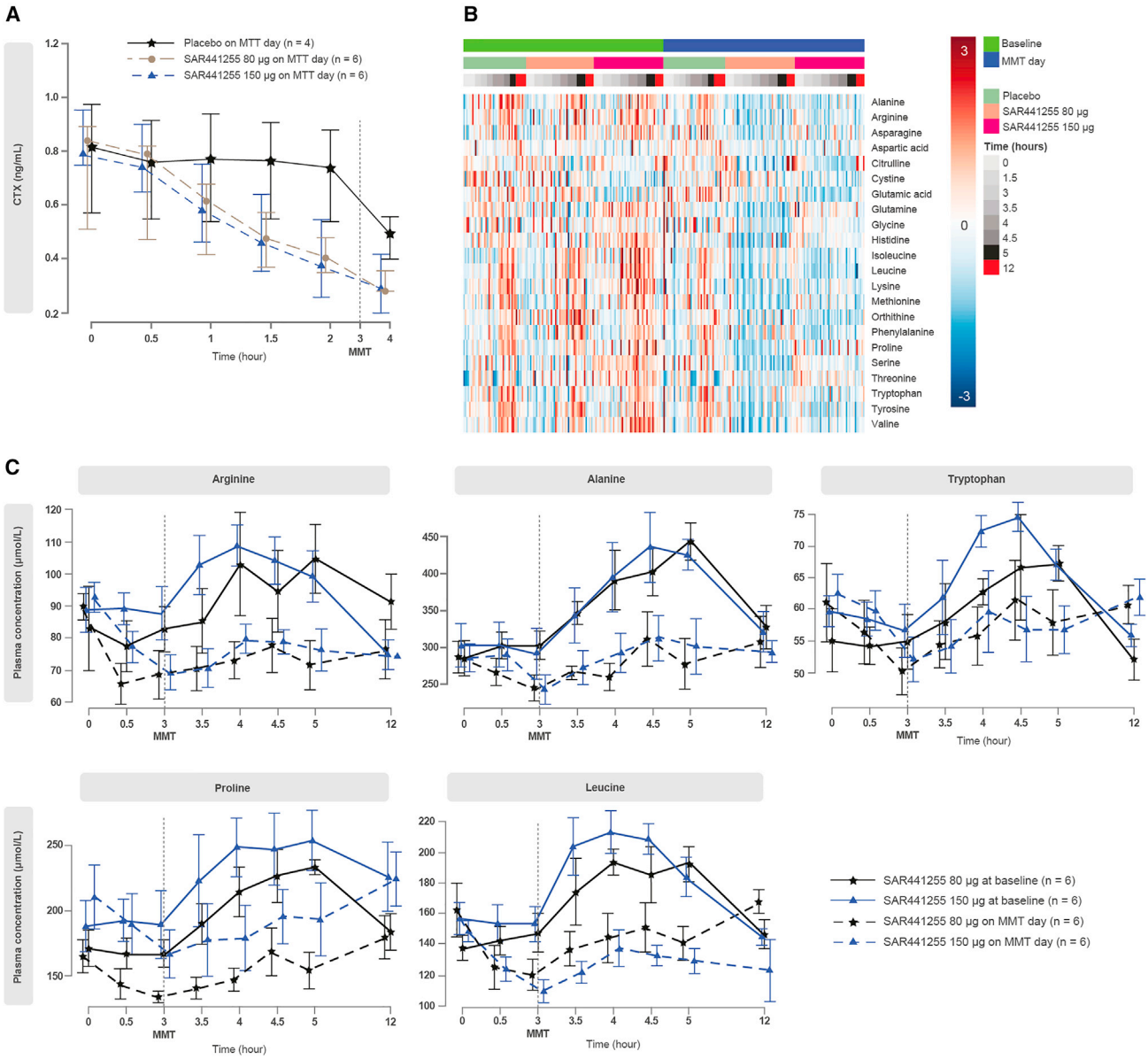

Figure 6. SAR441255 showed a substantial decrease in CTX and AA levels in humans

(A) Plasma concentrations of CTX following single doses of placebo and SAR441255 (80 and 150 µg dose groups).

(B and C) Heatmap of scaled AA levels (B) and representative individual AA plasma-concentration profiles for 5 selected AAs (C) at baseline (day –1, dashed lines) and on MMT day (day 1, solid lines) for 80 µg (black, n = 6) and 150 µg SAR441255 (red, n = 6) doses. Placebo data are not shown in (C). The MMT was administered at 3 h post-dose (i.e., 0 to 3 h and 12 h values are in the fasting state; 3.5 to 5 h values are in the fed state).

Values in (A) represent medians (interquartile range) and (C) represents means ± SEM. In (B), each row of the heatmap represents an AA, and each column represents a participant. The color code in the heatmap represents the relative concentration of each scaled AA (mean/SD): red and blue colors are mean increased and decreased levels of each AA, respectively. The scaled AA levels range from high (mean + 3 × SD, dark red) to middle (mean, white) to low (mean – 3 × SD, dark blue). The mean of scaled data is 0 and the SD = 1; hence, the range shown is between –3 and +3. On top of the map, the first color bar represents the study visit (light green for AA levels at baseline and blue for AA levels on MMT day). The second color bar represents the treatment groups and the third bar the time points (h) on each day.

observed in obese mice and monkeys. These results indicate that addition of GIP activity into dual GLP-1 and GCG receptor agonism provides improved effects on weight loss and glycemic control while protecting against the diabetogenic risk of chronic GCGR agonism. Importantly, the addition of the GIP component allows an increased potency of the agonist at the GCGR.

The data reported here for SAR441255 in diabetic obese monkeys and previously for a separate triagonist (peptide 12) by Evers and colleagues (Evers et al., 2020) suggest that the interplay of the three receptors involved allows some greater flexibility in finding an appropriate receptor balance for a highly efficient triple agonist targeting both body weight and glucose

control. All three principles contribute to body weight loss while two principles (GLP-1/GIP) augment blood glucose lowering. SAR441255 and peptide 12 are two triple agonists that have differing activation profiles. Despite these differences in their receptor activity, both demonstrate a consistent reduction in body weight while maintaining or improving HbA1c levels.

Recent clinical data for two dual GLP-1R/GCGR dual agonists highlight the challenges of determining the appropriate potency balance at the different receptors in these compounds to provide both substantial body weight loss and improved glucose control. In one dose-ranging trial, the Fc fusion conjugate JNJ-64565111 with high potency at the GCG receptor showed a significant reduction in body weight (mean change −7.2% versus placebo at the highest dose) after 12 weeks in obese diabetic patients without any improvement in glycemic control (Di Prospero et al., 2021). In the second trial, the acylated peptide cotadutide with lower potency at the GCG receptor (Henderson et al., 2016) showed weight loss (mean change −5.0% versus baseline) along with reduced HbA1c levels at the highest dose after 54 weeks in obese or overweight diabetic patients (Nahra et al., 2021). Compared with the selective GLP-1R agonist liraglutide comparator, cotadutide showed greater weight loss (mean difference −1.7%) without any difference in HbA1c levels after 54 weeks. These results underline the importance of the initially chosen receptor balance on subsequent clinical outcomes. In addition, recent clinical data with the dual GIP/GLP-1R agonist tirzepatide highlight how combining GIP and GLP-1 receptor agonism in a single compound can provide a greater effect on glucose levels and body weight control than with selective GLP-1R agonists alone in patients with T2D who are overweight or obese (Frías et al., 2021). This ongoing understanding of the potential benefits of multiple co-agonist incretin combinations is likely to lead to enhanced treatment options for patients in a range of metabolic disorders.

To our knowledge, this is the first time a preclinical monkey model in conjunction with PET imaging was used to assess *in vivo* receptor occupancy and quantify target engagement of a novel multiagonist at the GLP-1 and GCG receptors. To further understand receptor occupancy of SAR441255 in humans, an analogous PET study using these selective PET tracers for the GLP-1 and GCG receptors would provide valuable information. The usefulness of this imaging approach to assess receptor occupancy was recently reported in individuals with T2D who were treated with the dual GLP-1/GCG receptor agonist SAR425899 (Eriksson et al., 2020). A recently reported PET tracer for the GIP receptor could also be included in such a study to assess target engagement at this third receptor (Eriksson et al., 2021).

Simultaneous target engagement of GIP, GCG, and GLP-1 receptors in humans was also demonstrated in the first-in-human study. Using previously established biomarkers (CTX, AAs) for GIPR and GCGR activation, we highlighted the dynamic changes in CTX-1 levels and AA concentrations that occur following administration of SAR441255 in both the fasting and postprandial state. These data suggest that the effects observed in preclinical *in vivo* studies are translatable to human. While the initial human data in a relatively small number of healthy subjects are promising, further comparative trials in larger populations of people with T2D and obesity are required to confirm the therapeutic potential of this new GLP-1, GIP, and GCG receptor triagonist, particularly in comparison with existing selective GLP-1, dual GLP-1/GCG, and dual GLP-1/GIP receptor agonists.

Limitations of study

Several limitations in the reported work should be considered. In the diabetic obese cynomolgus monkey study, the small size of each group (7–10 animals) limited our ability to detect statistically significant differences between the active treatment groups for many of the evaluated parameters. In addition, it was logistically not possible to include a dual GLP-1R/GIPR agonist comparator group in this study. In addition, the PET tracer studies were conducted in lean cynomolgus monkeys, while the glycemic and metabolic effects of SAR441255 were evaluated in obese diabetic animals. Differences in receptor expression between lean and diabetic obese animals may have had an impact on the results. The lack of a suitable PET tracer with sufficient potency to assess GIP receptor occupancy also precluded quantitative assessment of target engagement at this receptor by SAR411255. However, the observed biomarker findings for CTX levels provided reasonable qualitative evidence for GIP receptor engagement by SAR441255.

Several limitations of the single-dose first-in-human study are recognized. First, only a small number of healthy volunteers were included due to the primary focus on assessing the safety and tolerability of SAR441255. While the preliminary pharmacodynamic results show clear improvement in glycemic parameters (FPG, PPG) following treatment with this GLP-1, GIP, and GCG receptor triagonist, the results can potentially be confounded by the GLP-1R-mediated inhibition of gastric emptying. Second, uncertainty remains concerning the effect of SAR441255 on glycemic parameters and tolerability with repeated dosing in the relevant patient population of people with T2D and/or obesity. The effects of SAR441255 on food intake or energy expenditure were also not evaluated in this study.

STAR★METHODS

Detailed methods are provided in the online version of this paper and include the following:

- KEY RESOURCES TABLE
- RESOURCE AVAILABILITY
  - Lead contact
  - Materials availability
  - Data and code availability
- EXPERIMENTAL MODEL AND SUBJECT DETAILS
  - Cell line
  - Animals
  - Human subjects
- METHOD DETAILS
  - Solid phase peptide synthesis of SAR441255
  - *In vitro* cellular assays for GLP-1, GIP and GCG receptor activation
  - Diet-Induced Obese (DIO) mouse study
  - Effects of SAR441255 on body weight in obese, diabetic cynomolgus monkeys
  - PET imaging and analysis in lean cynomolgus monkeys

- Cardiovascular safety of SAR441255 in lean telemetered cynomolgus monkeys
- Phase 1 study in healthy lean-to-overweight subjects
- QUANTIFICATION AND STATISTICAL ANALYSIS
  - Calculations
  - Statistical analysis
- ADDITIONAL RESOURCES

SUPPLEMENTAL INFORMATION

Supplemental information can be found online at https://doi.org/10.1016/j.cmet.2021.12.005.

ACKNOWLEDGMENTS

The authors would like to thank Martin Lorenz for his efforts during the starting phase of the research project, along with Ziyu Li, Thomas Hardt, Julia Diether, Ruediger Noll, Sabine Apel, and Ulrike Bewersdorf for the *in vitro* measurements and Stefania Pfeiffer-Marek for formulation support. Manfred Schmalz and the team at Kunming Biomed International (KBI) are thanked for planning and conducting *in vivo* experiments. The Uppsala University Hospital PET center and the Uppsala University Preclinical PET/MRI Platform team are thanked for the PET experiments. Thanks to Dominique Tytgat for translational pharmacokinetic/pharmacodynamic modeling; Fabienne Schumacher, Nian Tian, and Nadine Almeras for clinical support; and Kathrin Heermeier for clinical biomarker support. The authors would like to thank Cardiabase (Banook Group, Nancy, France), who were responsible for the analyses of the Holter recordings and provision of the Holter-derived data. Writing assistance during the manuscript preparation was provided by Dan Quinlan from Oberon Ltd (London, United Kingdom), funded by Sanofi. All studies were funded by Sanofi Germany.

AUTHOR CONTRIBUTIONS

The corresponding authors M.B. and A.K. confirm full access to data and final responsibility for the decision to submit for publication. M.B., M.W., A.E., and K.L. were responsible for the design, synthesis, and selection of SAR441255. M.B., R.E., T.H., T. Kloeckener, C.M., G.D., Y.D.-B., T. Kissner, and A.K. were responsible for the preclinical *in vitro* and *in vivo* studies and manuscript preparation. M.B., M.W., O.E., I.V., S.P., and L.J. were responsible for design, conduct, and data analysis of the PET study. I.N., C.E., C.J., F.R., and A.N. were responsible for the Phase 1 study design, data analysis, and manuscript preparation. J.G., H.-P.P., and I.A. were responsible for the biomarker design, biomarker data analysis, and manuscript preparation. A.N., N.P., and A.K. were responsible for the development of SAR441255. W.B.S. was the principal investigator at the New Orleans Center for Clinical Research, University of Tennessee Medical Center, responsible for the recruitment, treatment, and surveillance of study participants as well as the practical conduct of the Phase 1 trial.

DECLARATION OF INTERESTS

M.B., M.W., R.E., A.E., T.H., T. Kloeckener, K.L., C.M., G.D., Y.D.-B., T. Kissner, I.N., C.E., C.J., F.R., J.G., H.-P.P., I.A., N.P., A.N., and A.K. were employees of Sanofi when the studies were conducted and may hold shares and/or stock options in the company. M.B., M.W., A.E., and K.L. are inventors on the patent application WO2018100135 containing SAR441255. O.E. and S.P. are employees of Antaros Medical AB, which received payment for the practical conduct of the PET study. Otherwise, they declare no competing interests. L.J. is co-founder, co-owner, and employee of Antaros Medical AB, which received payment for the practical conduct of the PET study. Otherwise, L.J. declares no competing interests. I.V. is an employee of Uppsala University Hospital, which received payment for the practical conduct of the PET study. I.V. declares no competing interests. W.B.S. was the principal investigator of the study conducted at the MDNOCCR Alliance for Multispecialty Research (AMR)/DBA NOCCR (New Orleans Center for Clinical Research), Knoxville, Tennessee, and received payment for the practical conduct of the study. No payment was received for the preparation of this manuscript. No other potential conflicts of interest relevant to this article were reported.

Received: May 3, 2021
Revised: August 13, 2021
Accepted: December 6, 2021
Published: December 20, 2021

REFERENCES

Ahrén, B., Schweizer, A., Dejager, S., Dunning, B.E., Nilsson, P.M., Persson, M., and Foley, J.E. (2009). Vildagliptin enhances islet responsiveness to both hyper- and hypoglycemia in patients with type 2 diabetes. J. Clin. Endocrinol. Metab. *94*, 1236–1243.

Aliu, E., Kanungo, S., and Arnold, G.L. (2018). Amino acid disorders. Ann. Transl. Med. *6*, 471.

Ambery, P., Parker, V.E., Stumvoll, M., Posch, M.G., Heise, T., Plum-Moerschel, L., Tsai, L.F., Robertson, D., Jain, M., Petrone, M., et al. (2018a). MEDI0382, a GLP-1 and glucagon receptor dual agonist, in obese or overweight patients with type 2 diabetes: a randomised, controlled, double-blind, ascending dose and phase 2a study. Lancet *391*, 2607–2618.

Ambery, P.D., Klammt, S., Posch, M.G., Petrone, M., Pu, W., Rondinone, C., Jermutus, L., and Hirshberg, B. (2018b). MEDI0382, a GLP-1/glucagon receptor dual agonist, meets safety and tolerability endpoints in a single-dose, healthy-subject, randomized, Phase 1 study. Br. J. Clin. Pharmacol. *84*, 2325–2335.

Bech, E.M., Pedersen, S.L., and Jensen, K.J. (2018). Chemical strategies for half-life extension of biopharmaceuticals: lipidation and its alternatives. ACS Med. Chem. Lett. *9*, 577–580.

Becker, R.H., Stechl, J., Steinstraesser, A., Golor, G., and Pellissier, F. (2015). Lixisenatide reduces postprandial hyperglycaemia via gastrostatic and insulinotropic effects. Diabetes Metab. Res. Rev. *31*, 610–618.

Bergmann, N.C., Lund, A., Gasbjerg, L.S., Jørgensen, N.R., Jessen, L., Hartmann, B., Holst, J.J., Christensen, M.B., Vilsbøll, T., and Knop, F.K. (2019). Separate and combined effects of GIP and GLP-1 infusions on bone metabolism in overweight men without diabetes. J. Clin. Endocrinol. Metab. *104*, 2953–2960.

Bhat, V.K., Kerr, B.D., Flatt, P.R., and Gault, V.A. (2013a). A novel GIP-oxyntomodulin hybrid peptide acting through GIP, glucagon and GLP-1 receptors exhibits weight reducing and anti-diabetic properties. Biochem. Pharmacol. *85*, 1655–1662.

Bhat, V.K., Kerr, B.D., Vasu, S., Flatt, P.R., and Gault, V.A. (2013b). A DPP-IV-resistant triple-acting agonist of GIP, GLP-1 and glucagon receptors with potent glucose-lowering and insulinotropic actions in high-fat-fed mice. Diabetologia *56*, 1417–1424.

Boden, G., Rezvani, I., and Owen, O.E. (1984). Effects of glucagon on plasma amino acids. J. Clin. Invest. *73*, 785–793.

Chabenne, J.R., DiMarchi, M.A., Gelfanov, V.M., and DiMarchi, R.D. (2010). Optimization of the native glucagon sequence for medicinal purposes. J. Diabetes Sci. Technol. *4*, 1322–1331.

Christensen, M., Vedtofte, L., Holst, J.J., Vilsbøll, T., and Knop, F.K. (2011). Glucose-dependent insulinotropic polypeptide: a bifunctional glucose-dependent regulator of glucagon and insulin secretion in humans. Diabetes *60*, 3103–3109.

Christensen, M.B., Calanna, S., Holst, J.J., Vilsbøll, T., and Knop, F.K. (2014). Glucose-dependent insulinotropic polypeptide: blood glucose stabilizing effects in patients with type 2 diabetes. J. Clin. Endocrinol. Metab. *99*, E418–E426.

Christensen, M.B., Lund, A., Calanna, S., Jørgensen, N.R., Holst, J.J., Vilsbøll, T., and Knop, F.K. (2018). Glucose-dependent insulinotropic polypeptide (GIP) inhibits bone resorption independently of insulin and glycemia. J. Clin. Endocrinol. Metab. *103*, 288–294.

Christensen, M.B., Lund, A.B., Jørgensen, N.R., Holst, J.J., Vilsbøll, T., and Knop, F.K. (2020). Glucose-dependent insulinotropic polypeptide (GIP)

reduces bone resorption in patients with type 2 diabetes. J. Endocr. Soc. *4*, a097.

Clemmensen, C., Finan, B., Müller, T.D., DiMarchi, R.D., Tschöp, M.H., and Hofmann, S.M. (2019). Emerging hormonal-based combination pharmacotherapies for the treatment of metabolic diseases. Nat. Rev. Endocrinol. *15*, 90–104.

Coskun, T., Sloop, K.W., Loghin, C., Alsina-Fernandez, J., Urva, S., Bokvist, K.B., Cui, X., Briere, D.A., Cabrera, O., Roell, W.C., et al. (2018). LY3298176, a novel dual GIP and GLP-1 receptor agonist for the treatment of type 2 diabetes mellitus: From discovery to clinical proof of concept. Mol. Metab. *18*, 3–14.

Day, J.W., Ottaway, N., Patterson, J.T., Gelfanov, V., Smiley, D., Gidda, J., Findeisen, H., Bruemmer, D., Drucker, D.J., Chaudhary, N., et al. (2009). A new glucagon and GLP-1 co-agonist eliminates obesity in rodents. Nat. Chem. Biol. *5*, 749–757.

Day, J.W., Gelfanov, V., Smiley, D., Carrington, P.E., Eiermann, G., Chicchi, G., Erion, M.D., Gidda, J., Thornberry, N.A., Tschöp, M.H., et al. (2012). Optimization of co-agonism at GLP-1 and glucagon receptors to safely maximize weight reduction in DIO-rodents. Biopolymers *98*, 443–450.

Deacon, C.F. (2004). Circulation and degradation of GIP and GLP-1. Horm. Metab. Res. *36*, 761–765.

Di Prospero, N.A., Yee, J., Frustaci, M.E., Samtani, M.N., Alba, M., and Fleck, P. (2021). Efficacy and safety of glucagon-like peptide-1/glucagon receptor co-agonist JNJ-64565111 in individuals with type 2 diabetes mellitus and obesity: a randomized dose-ranging study. Clin. Obes. *11*, e12433.

Ding, K.H., Shi, X.M., Zhong, Q., Kang, B., Xie, D., Bollag, W.B., Bollag, R.J., Hill, W., Washington, W., Mi, Q.S., et al. (2008). Impact of glucose-dependent insulinotropic peptide on age-induced bone loss. J. Bone Miner. Res. *23*, 536–543.

Drucker, D.J. (2018). Mechanisms of action and therapeutic application of glucagon-like peptide-1. Cell Metab. *27*, 740–756.

Elvert, R., Bossart, M., Herling, A.W., Weiss, T., Zhang, B., Kannt, A., Wagner, M., Haack, T., Evers, A., Dudda, A., et al. (2018a). Team players or opponents: Coadministration of selective glucagon and GLP-1 receptor agonists in obese diabetic monkeys. Endocrinology *159*, 3105–3119.

Elvert, R., Herling, A.W., Bossart, M., Weiss, T., Zhang, B., Wenski, P., Wandschneider, J., Kleutsch, S., Butty, U., Kannt, A., et al. (2018b). Running on mixed fuel-dual agonistic approach of GLP-1 and GCG receptors leads to beneficial impact on body weight and blood glucose control: a comparative study between mice and non-human primates. Diabetes Obes. Metab. *20*, 1836–1851.

Eriksson, O., Velikyan, I., Haack, T., Bossart, M., Evers, A., Laitinen, I., Larsen, P.J., Plettenburg, O., Takano, A., Halldin, C., et al. (2019). Assessment of glucagon receptor occupancy by positron emission tomography in non-human primates. Sci. Rep. *9*, 14960.

Eriksson, O., Haack, T., Hijazi, Y., Teichert, L., Tavernier, V., Laitinen, I., Berglund, J.E., Antoni, G., Velikyan, I., Johansson, L., et al. (2020). Receptor occupancy of dual glucagon-like peptide 1/glucagon receptor agonist SAR425899 in individuals with type 2 diabetes. Sci. Rep. *10*, 16758.

Eriksson, O., Velikyan, I., Haack, T., Bossart, M., Evers, A., Lorenz, K., Laitinen, I., Larsen, P.J., Plettenburg, O., Johansson, L., et al. (2021). Drug occupancy assessment at the glucose-dependent insulinotropic polypeptide receptor by positron emission tomography. Diabetes *70*, 842–853.

European Medicines Agency (2009). Committee for Medicinal Products for Human Use (CHMP) Assessment Report for Victozia (liraglutide). https://www.ema.europa.eu/en/documents/assessment-report/victoza-epar-public-assessment-report_en.pdf.

Everman, S., Meyer, C., Tran, L., Hoffman, N., Carroll, C.C., Dedmon, W.L., and Katsanos, C.S. (2016). Insulin does not stimulate muscle protein synthesis during increased plasma branched-chain amino acids alone but still decreases whole body proteolysis in humans. Am. J. Physiol. Endocrinol. Metab. *311*, E671–E677.

Evers, A., Bossart, M., Pfeiffer-Marek, S., Elvert, R., Schreuder, H., Kurz, M., Stengelin, S., Lorenz, M., Herling, A., Konkar, A., et al. (2018). Dual glucagon-like peptide 1 (GLP-1)/glucagon receptor agonists specifically optimized for multidose formulations. J. Med. Chem. *61*, 5580–5593.

Evers, A., Pfeiffer-Marek, S., Bossart, M., Heubel, C., Stock, U., Tiwari, G., Gebauer, B., Elshorst, B., Pfenninger, A., Lukasczyk, U., et al. (2019). Peptide optimization at the drug discovery-development interface: tailoring of physicochemical properties toward specific formulation requirements. J. Pharm. Sci. *108*, 1404–1414.

Evers, A., Haack, T., Lorenz, M., Bossart, M., Elvert, R., Henkel, B., Stengelin, S., Kurz, M., Glien, M., Dudda, A., et al. (2017). Design of novel exendin-based dual glucagon-like peptide 1 (GLP-1)/glucagon receptor agonists. J. Med. Chem. *60*, 4293–4303.

Evers, A., Pfeiffer-Marek, S., Bossart, M., Elvert, R., Lorenz, K., Heubel, C., Garea, A.V., Schroeter, K., Riedel, J., Stock, U., et al. (2020). Multiparameter peptide optimization toward stable triple agonists for the treatment of diabetes and obesity. Adv. Ther. *3*, 2000052.

Finan, B., Ma, T., Ottaway, N., Müller, T.D., Habegger, K.M., Heppner, K.M., Kirchner, H., Holland, J., Hembree, J., Raver, C., et al. (2013). Unimolecular dual incretins maximize metabolic benefits in rodents, monkeys, and humans. Sci. Transl. Med. *5*, 209ra151.

Finan, B., Yang, B., Ottaway, N., Smiley, D.L., Ma, T., Clemmensen, C., Chabenne, J., Zhang, L., Habegger, K.M., Fischer, K., et al. (2015). A rationally designed monomeric peptide triagonist corrects obesity and diabetes in rodents. Nat. Med. *21*, 27–36.

Finan, B., Müller, T.D., Clemmensen, C., Perez-Tilve, D., DiMarchi, R.D., and Tschöp, M.H. (2016). Reappraisal of GIP pharmacology for metabolic diseases. Trends Mol. Med. *22*, 359–376.

Frias, J.P., Bastyr, E.J., 3rd, Vignati, L., Tschöp, M.H., Schmitt, C., Owen, K., Christensen, R.H., and DiMarchi, R.D. (2017). The sustained effects of a dual GIP/GLP-1 receptor agonist, NNC0090-2746, in patients with type 2 diabetes. Cell Metab. *26*, 343–352.e2.

Frías, J.P., Davies, M.J., Rosenstock, J., Pérez Manghi, F.C., Fernández Landó, L., Bergman, B.K., Liu, B., Cui, X., and Brown, K.; SURPASS-2 Investigators (2021). Tirzepatide versus semaglutide once weekly in patients with type 2 diabetes. N. Engl. J. Med. *385*, 503–515.

Gasbjerg, L.S., Bari, E.J., Stensen, S., Hoe, B., Lanng, A.R., Mathiesen, D.S., Christensen, M.B., Hartmann, B., Holst, J.J., Rosenkilde, M.M., and Knop, F.K. (2021). Dose-dependent efficacy of the glucose-dependent insulinotropic polypeptide (GIP) receptor antagonist GIP(3-30)NH_2 on GIP actions in humans. Diabetes Obes. Metab. *23*, 68–74.

Gault, V.A., Bhat, V.K., Irwin, N., and Flatt, P.R. (2013). A novel glucagon-like peptide-1 (GLP-1)/glucagon hybrid peptide with triple-acting agonist activity at glucose-dependent insulinotropic polypeptide, GLP-1, and glucagon receptors and therapeutic potential in high fat-fed mice. J. Biol. Chem. *288*, 35581–35591.

Henderson, S.J., Konkar, A., Hornigold, D.C., Trevaskis, J.L., Jackson, R., Fritsch Fredin, M., Jansson-Löfmark, R., Naylor, J., Rossi, A., Bednarek, M.A., et al. (2016). Robust anti-obesity and metabolic effects of a dual GLP-1/glucagon receptor peptide agonist in rodents and non-human primates. Diabetes Obes. Metab. *18*, 1176–1190.

Heuvelman, V.D., Van Raalte, D.H., and Smits, M.M. (2020). Cardiovascular effects of glucagon-like peptide 1 receptor agonists: from mechanistic studies in humans to clinical outcomes. Cardiovasc. Res. *116*, 916–930.

International Hypoglycaemia Study Group (2015). Minimizing hypoglycemia in diabetes. Diabetes Care *38*, 1583–1591.

King, D.S., Fields, C.G., and Fields, G.B. (1990). A cleavage method which minimizes side reactions following Fmoc solid phase peptide synthesis. Int. J. Pept. Protein Res. *36*, 255–266.

Kleinert, M., Clemmensen, C., Hofmann, S.M., Moore, M.C., Renner, S., Woods, S.C., Huypens, P., Beckers, J., de Angelis, M.H., Schürmann, A., et al. (2018). Animal models of obesity and diabetes mellitus. Nat. Rev. Endocrinol. *14*, 140–162.

Kleinert, M., Sachs, S., Habegger, K.M., Hofmann, S.M., and Müller, T.D. (2019). Glucagon regulation of energy expenditure. Int. J. Mol. Sci. *20*, 5407.

Knudsen, L.B. (2010). Liraglutide: the therapeutic promise from animal models. Int. J. Clin. Pract. Suppl. 4–11.

Kraft, G., Coate, K.C., Winnick, J.J., Dardevet, D., Donahue, E.P., Cherrington, A.D., Williams, P.E., and Moore, M.C. (2017). Glucagon's effect on liver protein metabolism in vivo. Am. J. Physiol. Endocrinol. Metab. *313*, E263–E272.

Li, W., Kirchner, T., Ho, G., Bonilla, F., D'Aquino, K., Littrell, J., Zhang, R., Jian, W., Qiu, X., Zheng, S., et al. (2020). Amino acids are sensitive glucagon receptor-specific biomarkers for glucagon-like peptide-1 receptor/glucagon receptor dual agonists. Diabetes Obes. Metab. *22*, 2437–2450.

Logan, J., Fowler, J.S., Volkow, N.D., Wolf, A.P., Dewey, S.L., Schlyer, D.J., MacGregor, R.R., Hitzemann, R., Bendriem, B., Gatley, S.J., et al. (1990). Graphical analysis of reversible radioligand binding from time-activity measurements applied to [*N*-^{11}C-methyl]-(-)-cocaine PET studies in human subjects. J. Cereb. Blood Flow Metab. *10*, 740–747.

Lorenz, M., Pfeiffer, C., Steinsträsser, A., Becker, R.H., Rütten, H., Ruus, P., and Horowitz, M. (2013). Effects of lixisenatide once daily on gastric emptying in type 2 diabetes–relationship to postprandial glycemia. Regul. Pept. *185*, 1–8.

Lorenz, M., Lawson, F., Owens, D., Raccah, D., Roy-Duval, C., Lehmann, A., Perfetti, R., and Blonde, L. (2017). Differential effects of glucagon-like peptide-1 receptor agonists on heart rate. Cardiovasc. Diabetol. *16*, 6.

Madsen, A.N., Hansen, G., Paulsen, S.J., Lykkegaard, K., Tang-Christensen, M., Hansen, H.S., Levin, B.E., Larsen, P.J., Knudsen, L.B., Fosgerau, K., and Vrang, N. (2010). Long-term characterization of the diet-induced obese and diet-resistant rat model: a polygenetic rat model mimicking the human obesity syndrome. J. Endocrinol. *206*, 287–296.

Marathe, C.S., Rayner, C.K., Jones, K.L., and Horowitz, M. (2013). Relationships between gastric emptying, postprandial glycemia, and incretin hormones. Diabetes Care *36*, 1396–1405.

Marigliano, M., Casu, A., Bertera, S., Trucco, M., and Bottino, R. (2011). Hemoglobin A1C percentage in nonhuman primates: a useful tool to monitor diabetes before and after porcine pancreatic islet xenotransplantation. J. Transplant. *2011*, 965605.

Maselli, D.B., and Camilleri, M. (2021). Effects of GLP-1 and Its analogs on gastric physiology in diabetes mellitus and obesity. Adv. Exp. Med. Biol. *1307*, 171–192.

McCluskey, J.T., Hamid, M., Guo-Parke, H., McClenaghan, N.H., Gomis, R., and Flatt, P.R. (2011). Development and functional characterization of insulin-releasing human pancreatic beta cell lines produced by electrofusion. J. Biol. Chem. *286*, 21982–21992.

Mroz, P.A., Finan, B., Gelfanov, V., Yang, B., Tschöp, M.H., DiMarchi, R.D., and Perez-Tilve, D. (2019). Optimized GIP analogs promote body weight lowering in mice through GIPR agonism not antagonism. Mol. Metab. *20*, 51–62.

Mu, J., Qureshi, S.A., Brady, E.J., Muise, E.S., Candelore, M.R., Jiang, G., Li, Z., Wu, M.S., Yang, X., Dallas-Yang, Q., et al. (2012). Anti-diabetic efficacy and impact on amino acid metabolism of GRA1, a novel small-molecule glucagon receptor antagonist. PLoS ONE *7*, e49572.

Müller, T.D., Finan, B., Clemmensen, C., DiMarchi, R.D., and Tschöp, M.H. (2017). The new biology and pharmacology of glucagon. Physiol. Rev. *97*, 721–766.

Müller, T.D., Finan, B., Bloom, S.R., D'Alessio, D., Drucker, D.J., Flatt, P.R., Fritsche, A., Gribble, F., Grill, H.J., Habener, J.F., et al. (2019). Glucagon-like peptide 1 (GLP-1). Mol. Metab. *30*, 72–130.

Nahra, R., Wang, T., Gadde, K.M., Oscarsson, J., Stumvoll, M., Jermutus, L., Hirshberg, B., and Ambery, P. (2021). Effects of cotadutide on metabolic and hepatic parameters in adults with overweight or obesity and type 2 diabetes: a 54-week randomized phase 2b study. Diabetes Care *44*, 1433–1442.

Näslund, E., Bogefors, J., Skogar, S., Grybäck, P., Jacobsson, H., Holst, J.J., and Hellström, P.M. (1999). GLP-1 slows solid gastric emptying and inhibits insulin, glucagon, and PYY release in humans. Am. J. Physiol. *277*, R910–R916.

Nauck, M.A., Kemmeries, G., Holst, J.J., and Meier, J.J. (2011). Rapid tachyphylaxis of the glucagon-like peptide 1-induced deceleration of gastric emptying in humans. Diabetes *60*, 1561–1565.

Nauck, M.A., Quast, D.R., Wefers, J., and Meier, J.J. (2021). GLP-1 receptor agonists in the treatment of type 2 diabetes - state-of-the-art. Mol. Metab. *46*, 101102.

Nissen, A., Christensen, M., Knop, F.K., Vilsbøll, T., Holst, J.J., and Hartmann, B. (2014). Glucose-dependent insulinotropic polypeptide inhibits bone resorption in humans. J. Clin. Endocrinol. Metab. *99*, E2325–E2329.

Nissen, A., Marstrand, S., Skov-Jeppesen, K., Bremholm, L., Hornum, M., Andersen, U.B., Holst, J.J., Rosenkilde, M.M., and Hartmann, B. (2019). A pilot study showing acute inhibitory effect of GLP-1 on the bone resorption marker CTX in humans. JBMR Plus *3*, e10209.

Okamoto, H., Kim, J., Aglione, J., Lee, J., Cavino, K., Na, E., Rafique, A., Kim, J.H., Harp, J., Valenzuela, D.M., et al. (2015). Glucagon receptor blockade with a human antibody normalizes blood glucose in diabetic mice and monkeys. Endocrinology *156*, 2781–2794.

Okamoto, H., Cavino, K., Na, E., Krumm, E., Kim, S.Y., Cheng, X., Murphy, A.J., Yancopoulos, G.D., and Gromada, J. (2017). Glucagon receptor inhibition normalizes blood glucose in severe insulin-resistant mice. Proc. Natl. Acad. Sci. USA *114*, 2753–2758.

Owens, D.R., Monnier, L., and Bolli, G.B. (2013). Differential effects of GLP-1 receptor agonists on components of dysglycaemia in individuals with type 2 diabetes mellitus. Diabetes Metab. *39*, 485–496.

Perry, R.J., Zhang, D., Guerra, M.T., Brill, A.L., Goedeke, L., Nasiri, A.R., Rabin-Court, A., Wang, Y., Peng, L., Dufour, S., et al. (2020). Glucagon stimulates gluconeogenesis by INSP3R1-mediated hepatic lipolysis. Nature *579*, 279–283.

Petersen, K.M., Bøgevig, S., Holst, J.J., Knop, F.K., and Christensen, M.B. (2018). Hemodynamic effects of glucagon: a literature review. J. Clin. Endocrinol. Metab. *103*, 1804–1812.

Portron, A., Jadidi, S., Sarkar, N., DiMarchi, R., and Schmitt, C. (2017). Pharmacodynamics, pharmacokinetics, safety and tolerability of the novel dual glucose-dependent insulinotropic polypeptide/glucagon-like peptide-1 agonist RG7697 after single subcutaneous administration in healthy subjects. Diabetes Obes. Metab. *19*, 1446–1453.

Raun, K., von Voss, P., Gotfredsen, C.F., Golozoubova, V., Rolin, B., and Knudsen, L.B. (2007). Liraglutide, a long-acting glucagon-like peptide-1 analog, reduces body weight and food intake in obese candy-fed rats, whereas a dipeptidyl peptidase-IV inhibitor, vildagliptin, does not. Diabetes *56*, 8–15.

Romero-Díaz, C., Duarte-Montero, D., Gutiérrez-Romero, S.A., and Mendivil, C.O. (2021). Diabetes and bone fragility. Diabetes Ther. *12*, 71–86.

Rosenstock, J., Wysham, C., Frías, J.P., Kaneko, S., Lee, C.J., Fernández Landó, L., Mao, H., Cui, X., Karanikas, C.A., and Thieu, V.T. (2021). Efficacy and safety of a novel dual GIP and GLP-1 receptor agonist tirzepatide in patients with type 2 diabetes (SURPASS-1): a double-blind, randomised, phase 3 trial. Lancet *398*, 143–155.

Samms, R.J., Coghlan, M.P., and Sloop, K.W. (2020). How may GIP enhance the therapeutic efficacy of GLP-1? Trends Endocrinol. Metab. *31*, 410–421.

Schmitt, C., Portron, A., Jadidi, S., Sarkar, N., and DiMarchi, R. (2017). Pharmacodynamics, pharmacokinetics and safety of multiple ascending doses of the novel dual glucose-dependent insulinotropic polypeptide/glucagon-like peptide-1 agonist RG7697 in people with type 2 diabetes mellitus. Diabetes Obes. Metab. *19*, 1436–1445.

Seghieri, M., Christensen, A.S., Andersen, A., Solini, A., Knop, F.K., and Vilsbøll, T. (2018). Future perspectives on GLP-1 receptor agonists and GLP-1/glucagon receptor co-agonists in the treatment of NAFLD. Front. Endocrinol. (Lausanne) *9*, 649.

Selvaraju, R.K., Velikyan, I., Johansson, L., Wu, Z., Todorov, I., Shively, J., Kandeel, F., Korsgren, O., and Eriksson, O. (2013). In vivo imaging of the glucagonlike peptide 1 receptor in the pancreas with ^{68}Ga-labeled DO3A-exendin-4. J. Nucl. Med. *54*, 1458–1463.

Solloway, M.J., Madjidi, A., Gu, C., Eastham-Anderson, J., Clarke, H.J., Kljavin, N., Zavala-Solorio, J., Kates, L., Friedman, B., Brauer, M., et al. (2015). Glucagon couples hepatic amino acid catabolism to mTOR-dependent regulation of α-cell mass. Cell Rep. *12*, 495–510.

Sparre-Ulrich, A.H., Hansen, L.S., Svendsen, B., Christensen, M., Knop, F.K., Hartmann, B., Holst, J.J., and Rosenkilde, M.M. (2016). Species-specific action of (Pro3)GIP - a full agonist at human GIP receptors, but a partial agonist and competitive antagonist at rat and mouse GIP receptors. Br. J. Pharmacol. *173*, 27–38.

Sumida, Y., Yoneda, M., Ogawa, Y., Yoneda, M., Okanoue, T., and Nakajima, A. (2020). Current and new pharmacotherapy options for non-alcoholic steatohepatitis. Expert Opin. Pharmacother. *21*, 953–967.

Talsania, T., Anini, Y., Siu, S., Drucker, D.J., and Brubaker, P.L. (2005). Peripheral exendin-4 and peptide YY^{3-36} synergistically reduce food intake through different mechanisms in mice. Endocrinology *146*, 3748–3756.

Tillner, J., Posch, M.G., Wagner, F., Teichert, L., Hijazi, Y., Einig, C., Keil, S., Haack, T., Wagner, M., Bossart, M., and Larsen, P.J. (2019). A novel dual glucagon-like peptide and glucagon receptor agonist SAR425899: Results of randomized, placebo-controlled first-in-human and first-in-patient trials. Diabetes Obes. Metab. *21*, 120–128.

Tølbøl, K.S., Kristiansen, M.N., Hansen, H.H., Veidal, S.S., Rigbolt, K.T., Gillum, M.P., Jelsing, J., Vrang, N., and Feigh, M. (2018). Metabolic and hepatic effects of liraglutide, obeticholic acid and elafibranor in diet-induced obese mouse models of biopsy-confirmed nonalcoholic steatohepatitis. World J. Gastroenterol. *24*, 179–194.

Umapathysivam, M.M., Lee, M.Y., Jones, K.L., Annink, C.E., Cousins, C.E., Trahair, L.G., Rayner, C.K., Chapman, M.J., Nauck, M.A., Horowitz, M., and Deane, A.M. (2014). Comparative effects of prolonged and intermittent stimulation of the glucagon-like peptide 1 receptor on gastric emptying and glycemia. Diabetes *63*, 785–790.

Upadhyay, J., Polyzos, S.A., Perakakis, N., Thakkar, B., Paschou, S.A., Katsiki, N., Underwood, P., Park, K.H., Seufert, J., Kang, E.S., et al. (2018). Pharmacotherapy of type 2 diabetes: an update. Metabolism *78*, 13–42.

Urva, S., Coskun, T., Loghin, C., Cui, X., Beebe, E., O'Farrell, L., Briere, D.A., Benson, C., Nauck, M.A., and Haupt, A. (2020). The novel dual glucose-dependent insulinotropic polypeptide and glucagon-like peptide-1 (GLP-1) receptor agonist tirzepatide transiently delays gastric emptying similarly to selective long-acting GLP-1 receptor agonists. Diabetes Obes. Metab. *22*, 1886–1891.

Vaughan, K.L., and Mattison, J.A. (2016). Obesity and aging in humans and nonhuman primates: a mini-review. Gerontology *62*, 611–617.

Velikyan, I., Rosenstrom, U., and Eriksson, O. (2017). Fully automated GMP production of [^{68}Ga]Ga-DO3A-VS-Cys^{40}-Exendin-4 for clinical use. Am. J. Nucl. Med. Mol. Imaging *7*, 111–125.

Velikyan, I., Haack, T., Bossart, M., Evers, A., Laitinen, I., Larsen, P., Plettenburg, O., Johansson, L., Pierrou, S., Wagner, M., and Eriksson, O. (2019). First-in-class positron emission tomography tracer for the glucagon receptor. EJNMMI Res. *9*, 17.

Vilar-Gomez, E., Martinez-Perez, Y., Calzadilla-Bertot, L., Torres-Gonzalez, A., Gra-Oramas, B., Gonzalez-Fabian, L., Friedman, S.L., Diago, M., and Romero-Gomez, M. (2015). Weight loss through lifestyle modification significantly reduces features of nonalcoholic steatohepatitis. Gastroenterology *149*, 367–378.e5, quiz e14–e15.

Wagner, M., Doverfjord, J.G., Tillner, J., Antoni, G., Haack, T., Bossart, M., Laitinen, I., Johansson, L., Pierrou, S., Eriksson, O., and Velikyan, I. (2020). Automated GMP-compliant production of [^{68}Ga]Ga-DO3A-Tuna-2 for PET microdosing studies of the glucagon receptor in humans. Pharmaceuticals (Basel) *13*, 176.

Westberg-Rasmussen, S., Starup-Linde, J., Hermansen, K., Holst, J.J., Hartmann, B., Vestergaard, P., and Gregersen, S. (2017). Differential impact of glucose administered intravenously or orally on bone turnover markers in healthy male subjects. Bone *97*, 261–266.

Zaykov, A.N., Mayer, J.P., and DiMarchi, R.D. (2016). Pursuit of a perfect insulin. Nat. Rev. Drug Discov. *15*, 425–439.

Zhang, Q., Delessa, C.T., Augustin, R., Bakhti, M., Colldén, G., Drucker, D.J., Feuchtinger, A., Caceres, C.G., Grandl, G., Harger, A., et al. (2021). The glucose-dependent insulinotropic polypeptide (GIP) regulates body weight and food intake via CNS-GIPR signaling. Cell Metab. *33*, 833–844.e5.

STAR★METHODS

KEY RESOURCES TABLE

REAGENT or RESOURCE	SOURCE	IDENTIFIER
Chemicals, peptides, and recombinant proteins		
GLP-1(7-36)NH_2	Bachem	H-6795
GIP	Bachem	H-5645
GCG	Bachem	H-6790
BSA, essentially fatty acid free	MP Biomedicals	152401
SAR441255	In-house synthesis	See below
Peptide 12	In-house synthesis	(Evers et al., 2020)
Mouse dual GLP-1R/GCGR agonist	In-house synthesis	(Elvert et al., 2018b)
Monkey dual GLP-1R/GCGR agonist	In-house synthesis	(Elvert et al., 2018b)
Rink-Amide resin	Novabiochem	855120
Accutase solution	Sigma-Aldrich	A6964
Dimethylformamide (DMF)	Fisher Chemical	SP/2626/4l
20% piperidine/DMF	Sigma-Aldrich	80645
200 mM amino acid / 500 mM HBTU	ABCR	AB128869
2M DIPEA in NMP	Sigma-Aldrich	03439
Acetic acid	Fisher Chemical	A/0360/PB15
2,2,2-trifluoroethanol (TFE)	Alfa Aesar	A10788
Dichloromethane (DCM)	VWR	23373.320
5% DIPEA	VWR	84574.290
RPMI	GIBCO	Cat#: 21875
FBS Good	PAN Biotech	P40-38500
1% Pen/Strep	GIBCO	Cat#: 15140
HBSS solution	Invitrogen	Cat#: 14065
HEPES 20 mM solution	Invitrogen	Cat#: 15630
HEPES 15 mM	GIBCO	Cat#: 12509079
0.1% BSA	PAA Laboratories	Cat#: K35-002
IBMX solution	AppliChem	Cat#: A0695
DMEM	GIBCO	Cat#: 41965
Ham's F10	GIBCO	Cat#: 31550023
3% FCS	PAA Laboratories	A15-101
Biotin	Sigma-Aldrich	Cat#: B4501
Pantothenate	Sigma-Aldrich	Cat#: C8731
Human insulin	Sigma-Aldrich	Cat#: I9278
Dexamethasone	Sigma-Aldrich	Cat#: C4902
PPAR gamma agonist	Sigma-Aldrich	Cat#: R2408
Antibiotic-Antimycotic	Thermo Fisher Scientific	Cat#: 15240
L-thyroxine	Sigma-Aldrich	Cat#: T2376
Phosphate Buffered Saline (PBS) without calcium or magnesium	GIBCO	Cat#: 14190
Endothelial Cell Growth Medium MV	PromoCell	Cat#: C-22020, C-39225
Elecsys β-CrossLaps (CTX) reagent	Roche Diagnostics	Cat#: 11972308122
Ketamine hydrochloride (DIO study)	Bela-Pharm	Ketabel 100 mg/mL
Ketamine hydrochloride (PET study)	Apoteket	Cat#: 511519
50% glucose solution	Sigma	G8270-5kg
Glucose solution 300 mg/mL	Fresenius-Kabi	01-63-07001B

(*Continued on next page*)

Continued

REAGENT or RESOURCE	SOURCE	IDENTIFIER
Sevoflurane	AbbVie	007462
Acetic acid (glacial)	Fisher	A/0400/PB15
Glycerol 85% Ph. Eur.	Aug. Hedinger GmbH & Co. KG	040
L-Methionine	Sigma-Aldrich	M5308
Polysorbate 20 (PS20)	KLK Kolb	Kotilen-L/1
Critical commercial assays		
cAMP Gs dynamic Kit	Cisbio Corp	62AM4PEJ
Human Quantitative AA Kit	LabCorp	700068
HbA1c	Covance	HPLC
Monkey FGF-21 ELISA kit	Merck Millipore	EZHFGF21-19K
Human plasma CTX Elecsys β-CrossLaps/serum	Roche	ID 07026960190
Experimental models: Cell lines		
HEK293 cells expressing human/mouse/ monkey receptors	In-house synthesis	N/A
Human-derived pancreatic 1.1 B4 β-cells	ECACC	87092802
LIVERPOOL 50-donor pooled human cryopreserved hepatocytes	BioIVT	X008005
Human preadipocytes	Lonza	PT-5020
Experimental models: Organisms/strains		
DIO mice	Envigo RMS	N/A
Lean mice	Envigo RMS	N/A
Cynomolgus monkey	Kunming Biomed International	N/A
Cynomolgus monkey	Hartelust, Tilberg, the Netherlands	N/A
Cynomolgus monkey	Noveprim and Le Tamarinier, Mauritius	N/A
Software and algorithms		
PMOD 3.7 software	PMOD Technologies Ltd, Zurich, Switzerland	https://www.pmod.com/web
Phoenix WinNonlin	Certara, Princeton, NJ, USA	N/A
NOTOCORD-hem version 4.3.0	Notocord, Paris, France	N/A
Other		
Falcon 75 cm^2 flasks	BD Biosciences	Cat#: 353136
Falcon 175 cm^2 flasks	BD Biosciences	Cat#: 353112
96-well plate	Corning, Sigma-Aldrich	Cat#: CLS3694
384-well microplates	Greiner Bio-One	Cat#: 784904
Telemetry units	Data Sciences Company, MN, USA	Model L21
Bair Hugger warming unit	Arizant Healthcare, MN, USA	Model 505
[^{68}Ga]Ga-DO3A-Exendin4, radiotracer	In-house synthesis	(Selvaraju et al., 2013; Velikyan et al., 2017)
[^{68}Ga]Ga-DO3A-Tuna-2, radiotracer	In-house synthesis	(Velikyan et al., 2019; Wagner et al., 2020)

(*Continued on next page*)

Continued

REAGENT or RESOURCE	SOURCE	IDENTIFIER
Quantitative nuclear magnetic resonance (QNMR) spectrometry	EchoMRI Corporation Pte Ltd, Singapore	EchoMRI-100H
Dual energy X-ray absorptiometry (DEXA)	Hologic	Discovery QDR Series (Discovery Wi)
PET-CT scanner	GE Healthcare, Milwaukee, MI, USA	Discovery MI
Mouse high fat diet	Envigo	Cat#: TD97366
Mouse normal chow diet	Envigo	Teklad global 14% protein rodent maintenance diet
Monkey pelleted diet	SAFE, Augy, France	107C
Monkey high fat diet	Kunming Biomed International	N/A
Monkey normal diet	Kunming Biomed International	N/A

RESOURCE AVAILABILITY

Lead contact

Further information and requests for resources and reagents should be directed to and will be fulfilled by the Lead Contact, Martin Bossart (martin.bossart@sanofi.com).

Materials availability

This study did not generate new unique reagents or materials. Sequences of the monomeric triagonist SAR441255 and the mouse and monkey specific dual GLP-1/GCG receptor agonists (Elvert et al., 2018b) have been disclosed.

Data and code availability

- Data reported in this paper will be shared by the lead contact upon request
- This paper does not report original code.
- Any additional information required to reanalyze the data reported in this paper is available from the lead contact upon request.

EXPERIMENTAL MODEL AND SUBJECT DETAILS

Cell line

Human embryonic kidney (HEK293) cell lines stably expressing human, monkey or murine GLP-1, GIP and GCG receptors were generated at Sanofi, Frankfurt, Germany. Human adipocytes were purchased from Lonza, Basel, Switzerland. Human-derived 1.1 B4 pancreatic β-cells were purchased from the European Collection of Authenticated Cell Cultures (ECACC). The cells were cultured at 37°C, 5% CO_2 and 95% humidity in modified HBSS medium (HEK293 cells), RPMI medium (1.1B4 pancreatic β-cells) as described in detail later in the Method details.

Animals

The protocol for the mouse study was approved by the Animal Care and Use Committee of Covance Laboratories, Greenfield, Indiana, USA. Protocols for the three monkey studies were approved by the Institutional Animal Care and Use Committee of Kunming Biomed International (KBI, Yunnan Province, China), the Animal Ethics Committee of the Swedish Animal Welfare Agency and the Ethics Committee for the Protection of Laboratory Animals (CEPAL) of Sanofi (Sanofi-Aventis Recherche & Développement, Vitry-Alfortville, France), respectively. The animals received humane care according to the US Association for Assessment and Accreditation of Laboratory Animal Care, the Chinese National Advisory Committee for Laboratory Animal Research (NACLAR), and the French regulation (Décret 2013-118, dated February 1, 2013) implementing European Directive 2010/63 and European Convention ETS123. Animals were in generally good health.

Female lean and diet-induced obese (DIO) mice were purchased from Envigo RMS (Indianapolis, USA). Lean mice had been fed for 16 weeks with standard chow (Teklad Global Diets Rodent 2014 *ad libitum*) to serve as age matched controls while DIO mice had received a high fat diet (TD97366 *ad libitum*) to induce the DIO phenotype. Upon arrival at the study site (Covance Laboratories, Greenfield, Indiana, USA), the animals continued their respective diet for 38 days and at approximately 25 weeks of age were randomized into groups based on their body weight. Animals were grouped-housed (up to five animals per cage during the pre-dose phase and 4 animals per cage in the dosing phase) on a 12-h/12-h light-dark cycle in a controlled room (temperature 20 to 26°C, relative humidity range of 30 to 70%) with free access to food and water.

For the first monkey experiment, cynomolgus monkeys (*Macaca fascicularis*) born and raised in the KBI breeding facilities (Yunnan Province, China) were included in the study. Monkeys were individually housed in species- and size-appropriate cages on a 12-h/12-h light-dark cycle under controlled environmental conditions (temperature 20 to 26°C, relative humidity range of 30 to 70%, a minimum of 10 air changes/h) with free access to water. All monkeys received standard environmental enrichment with plastic chew toys, plastic balls, food puzzles and foraging trays. The animals were fed 3 meals per day consisting of 46.5 g of KBI proprietary standard monkey formula feed (extruded pellets) in the morning (9-10 am), one regular apple (150 g) in the afternoon (2-3 pm) and 100 g of KBI proprietary high fat diet (HFD) in the evening (4-5 pm). Food was withdrawn at 5 pm; hence, all the monkeys were always fasted overnight. After each feeding time, all the remaining food was withdrawn from the monkey and intake was determined by weighing the left-over food. Total energy intake (in kcal) was determined based on the total daily food intake.

For the second monkey experiment, lean cynomolgus monkeys (*Macaca fascicularis*) of Chinese origin were procured from Hartelust (Tilburg, the Netherlands) and included in a PET study. The animals were kept in groups of up to 10 individuals in a space of ~12-20 m^2 with combined indoor / outdoor living (at least 2 m^2 per monkey). The cage height was 2.5-3.7 m. Ten monkeys could sit in an outside enclosure (volume at least 20 m^2, height at least 2.5 m). Each monkey could move throughout the outside enclosure and was given the opportunity for activity and movements. Cages have a fixed interior with places where they could sit and things that they could climb on (e.g., recycled fire hoses, plastic pipes). Loose furnishings were replaced according to a certain schedule, including a bathtub, plastic bottles, plastic ball with holes in it (that could be filled with things that monkeys could peel off), wooden chopsticks, cardboard boxes and telephone directories (which they could tear apart). Monkeys had constant *ad libitum* access to the fodder (extruded pellets) and received fresh fruits and vegetables three times per day. The monkeys were kept together except when participating in experiments.

In the third monkey experiment, cynomolgus monkeys (*Macaca fascicularis*) were procured from Noveprim Ltd and Le Tamarinier (Mauritius) and included in a cardiovascular safety study. Upon arrival at the study site (Sanofi-Aventis Recherche & Développement, Alfortville, France) each animal was acclimated to an animal room for at least 3 weeks. Following surgical implantation of a telemetry device, each animal was kept in animal rooms for a recovery period of at least 2 weeks before being included in the study. During the weeks preceding the beginning of the study, the implanted monkeys were accustomed to the experimental conditions in a test room. For the study, 6 animals were selected from a colony of previously implanted cynomolgus monkeys. During the study, the animals were moved from animal rooms (19.9 m^2) to a dedicated test room where they were dual- or singly-housed in cages (2.2 m^2) according to social compatibility. Monkeys were housed in animal and test rooms on a 12-h/12-h light-dark cycle under controlled environmental conditions (temperature 20 to 24°C, relative humidity range of 40 to 70%, a minimum of 15 air changes/h) with free access to filtered water. All monkeys received standard environmental enrichment with toys. The animals were fed once a day at a fixed time with a certified pelleted diet (150 g limit). In addition, fresh fruits/vegetables, and delicacies (sunflower seeds and peanuts) were also provided everyday according to local procedure.

Human subjects

Trial design

A phase 1, randomized, double-blind, single-center, placebo-controlled trial was designed to evaluate the safety, tolerability, pharmacokinetics, and pharmacodynamics of single ascending subcutaneous (s.c.) doses of SAR441255 in lean to overweight healthy male or female adults. This study was conducted at New Orleans Center for Clinical Research, Knoxville, Tennessee, USA between April 2019 and September 2019. The study protocol was approved by an independent Ethics Committee and the trial was conducted in accordance with the guidelines established by the Declaration of Helsinki and the International Conference on Harmonization - Good Clinical Practice. Written informed consent was obtained from all study participants before study entry.

Participants

Eligible participants were healthy individuals aged 18 to 55 years with a body mass index (BMI) between 20 and 30 kg/m^2 (normal- to overweight). Participants were required to have normal blood pressure, pulse rate, body temperature, laboratory values, Holter and 12-lead electrocardiogram (ECG) results. No concomitant medication was allowed during the trial. A standard diet was maintained during the trial, including control of fluid and food intake. Completeness of meal intake was monitored and recorded.

METHOD DETAILS

Solid phase peptide synthesis of SAR441255

The solid phase synthesis was carried out on Rink-Amide resin (4-(2',4'-Dimethoxyphenyl-Fmoc-aminomethyl)-phenoxyacetamido-norleucylaminomethyl resin) (Novabiochem), 100-200 mesh, loading of 0.43 mmol/g on a Prelude peptide synthesizer (Protein Technologies). Fluorenylmethoxycarbonyl protecting group (Fmoc) protected natural amino acids (AAs) were purchased from Protein Technologies Inc., Novabiochem, Iris Biotech or Bachem. The following AAs were used as starting materials: Fmoc-L-Ala-OH, Fmoc-D-Ala-OH, Fmoc-L-Arg(Pbf)-OH, Fmoc-L-Asp(OtBu)-OH, Fmoc-L-Gln(Trt)-OH, Fmoc-L-Glu(OtBu)-OH, Fmoc-Gly-OH, Fmoc-L-His(Trt)-OH, Fmoc-L-Ile-OH, Fmoc-L-Leu-OH, Fmoc-L-Lys(Boc)-OH, Fmoc-L-Phe-OH, Fmoc-L-Pro-OH, Fmoc-L-Ser(tBu)-OH, Fmoc-L-Thr(tBu)-OH, Fmoc-L-Trp(Boc)-OH, Fmoc-Aib-OH. The Fmoc-synthesis strategy was applied with 2-(1H-benzotriazol-1-yl)-1,1,3,3-tetramethyluronium hexafluorophosphate (HBTU) / diisopropylethylamine (DIPEA)-activation. Dimethylformamide (DMF) (Fisher Chemical) was used as the solvent. For deprotection two runs of 20% piperidine/DMF (Sigma-Aldrich) for 2.5 min were followed by 7 DMF washes. Double couplings were done with a 2:5:10 mixture of 200 mM AA / 500 mM HBTU (ABCR) / 2M

DIPEA in NMP (Sigma-Aldrich) (20 min each) followed by 5 DMF washes. In position 14, Fmoc-Lys(Mmt)-OH and in position 1 Boc-His(Trt)-OH were used in the solid phase synthesis protocol. The monomethoxytrityl (Mmt) group was removed by repeated treatment with acetic acid (AcOH, Fisher Chemical) / 2,2,2-trifluoroethanol (TFE, Alfa Aesar) / dichloromethane (DCM, VWR) mixture (1:2:7) for 15 min at room temperature (RT), the resin then repeatedly washed with DCM, 5% DIPEA (VWR) in DCM and 5% DIPEA in DCM/DMF. Thereafter, Palm-γGlu-γGlu-OSu was coupled to the liberated amino group employing DIPEA as base. The peptide was cleaved from the resin with King's cocktail consisting of 82.5% trifluoroacetic acid (TFA), 5% phenol, 5% water, 5% thioanisole, 2.5% 1,2-ethanedithiol (EDT) (King et al., 1990). The crude peptide was then precipitated in cold diethyl ether, centrifuged, and lyophilized. Peptides were analyzed by analytical high-performance liquid chromatography (HPLC) and checked by electrospray ionization (ESI) mass spectrometry. The crude product was purified via preparative reversed-phase (RP)-HPLC on a Äkta Purifier System (Cytiva, formerly GE Healthcare), a Jasco semi-preparative HPLC System (Jasco) or an Agilent 1100 HPLC system (Agilent) on a Waters column (Sunfire Prep C18 ODB 5 μm 30 × 250 mm) using an acetonitrile/water (with 0.1% trifluoroacetic acid [TFA]) gradient. Product-containing fractions were collected and lyophilized to obtain the purified product, typically as TFA salt.

The purified peptide was analyzed on an 6230B Time of Flight (TOF) liquid chromatography/mass spectrometry (LC/MS) System using a Dual Agilent Jet Stream ESI source (Agilent). Liquid chromatography (LC) was performed on a ACQUITY UPLC CSH C18 1.7 μm (150 × 2.1 mm) column (Waters) at 50°C using a gradient of solvents: H_2O + 0.05% TFA: acetonitrile (ACN) + 0.035% TFA (flow 0.5 mL/min) (gradient: 80:20 (0 min) to 80:20 (3 min) to 25:75 (23 min) to 2:98 (23.5 min) to 2:98 (30.5 min) to 80:20 (31 min) to 80:20 (37 min)). The desired compound was detected with a retention time of 9.995 min (observed peptide mass 4863.67; calculated peptide mass 4863.63) with a purity of 95%.

In vitro cellular assays for GLP-1, GIP and GCG receptor activation

The ability of SAR441255 to activate GLP-1, GIP and glucagon (GCG) receptors was determined using functional assays, as described previously (Evers et al., 2017). The natural ligands for each receptor, namely GLP-1(7-36)NH_2, GCG and GIP(1-42), were used as the reference compounds. HEK293 cell lines stably expressing recombinant human, monkey or murine GLP-1, GIP or GCG receptors were used to measure elevation of cAMP levels in response to each compound. The HEK293 cells were grown in Falcon 175 cm^2 cell culture flasks (BD Biosciences) overnight to near confluence in medium [composition: Dulbecco's Modified Eagle Medium (DMEM, GIBCO) and 10% fetal bovine serum (FBS, PAN Biotech)] at 37°C, 5% CO_2 and 95% humidity. The medium was then removed, and cells were washed with phosphate buffered saline (PBS) lacking calcium and magnesium (GIBCO), followed by proteinase treatment with Accutase (Sigma-Aldrich). Detached cells were washed and resuspended in assay buffer [composition: Hank's balanced salt solution (HBSS, Invitrogen), 20 mM HEPES (Invitrogen), 0.1% bovine serum albumin (BSA, PAA Laboratories), and 2 mM 3-isobutyl-1-methylxanthine (IBMX, AppliChem)], and cellular density was determined. The cell suspension was then diluted to 400,000 cells/mL, and 25 μL aliquots were dispensed into the wells of 96-well plates (Corning, Sigma-Aldrich). For cAMP measurement, 25 μL of test compound in assay buffer was added to the wells, followed by incubation for 30 min at room temperature. cAMP levels generated following test compound stimulation were measured using a cAMP Gs dynamic kit (Cisbio), based on homogeneous time-resolved fluorescence (HTRF) technology, by following the manufacturer's instructions. After addition of HTRF reagents diluted in lysis buffer (kit components), the plates were incubated for 1 h, followed by measurement of the fluorescence ratio at 665/620 nm. The *in vitro* potency of the compounds was quantified by determining the concentrations that caused 50% activation of the maximal response (EC_{50}). Data were reported as the mean ± standard error of the mean (SEM) of three replicates.

The *in vitro* activity of SAR441255 was also studied in cell systems expressing endogenous levels of each receptor.

Endogenous GLP-1 receptor efficacy was assessed with 1.1B4 human pancreatic beta-cells (ECACC) (McCluskey et al., 2011) that were cultivated at 37°C, 5% CO_2 and 95% humidity in RPMI (GIBCO) supplemented with 10% FBS Good (PAN Biotech) and 1% Pen/Strep (GIBCO). For cAMP measurements, 7500 cells per well were dispensed in 25 μL assay buffer containing HBSS (Invitrogen), 20 mM HEPES (Invitrogen), 0.1% BSA (PAA Laboratories) on a 96-well plate (Corning, Sigma-Aldrich). For measurement of cAMP generation, 25 μL of test compound (1:10 serial dilutions) in assay buffer plus 2 mM IBMX (AppliChem) was added to each well of the 96-well plate, followed by incubation for 30 min at room temperature.

Endogenous GCG receptor efficacy was accessed with frozen primary human hepatocytes (BioIVT) that were thawed in assay buffer containing HBSS (Invitrogen), 20 mM HEPES (Invitrogen), and 0.01% BSA (PAA Laboratories). For cAMP measurements, 1000 cells per well were dispensed in 5 μL assay buffer containing HBSS (Invitrogen), 20 mM HEPES (Invitrogen), and 0.1% BSA (PAA Laboratories) on a 384-well plate (Greiner). For measurement of cAMP generation, 5 μL of test compound (1:5 or 1:8 serial dilutions) in assay buffer plus 2 mM IBMX (AppliChem) was added to each well of the 384-well plate, followed by incubation for 30 min at room temperature.

Lastly, endogenous GIP receptor efficacy was studied by monitoring lipolysis in human adipocytes differentiated *in vitro* from precursors.

Human preadipocytes (Lonza) were seeded on a 96-well plate (Corning) in Endothelial Cell Growth medium with supplement mix (PromoCell) as 28,000 cells per well. After 6 h, the medium was changed to differentiation medium consisting of DMEM (GIBCO), Ham's F10 (GIBCO), 15 mM HEPES (GIBCO), 3% FCS (PAA), 33 μM biotin (Sigma-Aldrich), 17 μM pantothenate (Sigma-Aldrich), 0.1 μM human insulin (Sigma-Aldrich), 1 μM dexamethasone (Sigma-Aldrich), 0.1 μM PPAR gamma agonist (Sigma-Aldrich), 0.6 x antibiotic-antimycotic (Thermo Fisher), 200 μM IBMX (AppliChem), and 0.01 μM L-thyroxine (Sigma-Aldrich). Preadipocytes were differentiated for at least 14 days and starved overnight before the lipolysis assay in starvation medium, consisting of DMEM (GIBCO),

Ham's F10 (GIBCO), 15 mM HEPES (GIBCO), 3% FCS (PAA), 33 μM biotin (Sigma-Aldrich), and 17 μM pantothenate (Sigma-Aldrich).

Serial dilutions (1:10) of compounds in adipocyte medium (DMEM (GIBCO), Ham's F10 (GIBCO), 15 mM HEPES (GIBCO), 3% FCS (PAA), 33 μM biotin (Sigma-Aldrich), 17 μM pantothenate (Sigma-Aldrich), 0.1 μM human insulin (Sigma-Aldrich), 1 μM dexamethasone (Sigma-Aldrich), 0.1 μM PPAR gamma agonist (Sigma-Aldrich), 0.6 x antibiotic-antimycotic (Thermo Fisher)) were added to the starved differentiated adipocytes and incubated at 37°C for 240 min. The amount of the produced free glycerol in each well was determined using free glycerol reagent (Sigma-Aldrich).

Diet-Induced Obese (DIO) mouse study

Ten lean C57BL/6NHsd and 75 DIO female mice were included in the study. At initiation of dosing, the animals were approximately 25 weeks of age, with body weights ranging from 22.4 to 24.8 g for the lean mice and from 42.0 to 53.7 g for the DIO mice. Animals were assigned to 8 treatment groups based on body weight.

At baseline, blood glucose concentrations were measured and blood for insulin analysis was collected. Body composition (determination of fat, lean, free water, and total water masses) was measured using quantitative nuclear magnetic resonance (QNMR) spectrometry (EchoMRI-100H) on the same day. Following randomization (day 1), animals received s.c. injections of SAR441255 (0.3, 1, 3, 10 or 30 μg/kg), vehicle control (PBS) or mouse dual GLP-1R/GCGR agonist (30 μg/kg) (Elvert et al., 2018b) administered twice daily (bid) for 28 days at a volume of 5 mL/kg. Animals were dosed only once on the day of scheduled necropsy.

The effectiveness of each treatment was determined by assessment of mortality, clinical observations, body weights, body fat content, and food consumption at follow-up. Blood was collected for measurements of blood glucose and insulin concentration, and clinical chemistry. QNMR spectrometry was performed on day 26 of the dosing phase.

One animal (vehicle control) died during QNMR blood collection on day 26. All other animals survived to day 28 when they were anesthetized via isoflurane, exsanguinated, and necropsied. Daily body weights and food consumption were reported until day 26 due to an animal death and collection errors for body weight and food consumption on days 27 and 28. The amount of food consumed by each cage of animals (four per cage) was estimated by measuring the full and empty feeder weights daily during the dosing phase. Consumption was calculated as grams per animal per day.

Blood for blood glucose measurements was collected via a tail clip on day 1 and day 26 of the dosing phase at 0 h (pre-dose) and 1, 2, 3, 4, 6, and 24 h post-dose. The 24-h sample was collected prior to dosing on day 2, and the 0-h, 24-h, and day 26 samples were collected prior to any other in-life activities. Blood for insulin measurement was collected from non-fasted animals via tail clip on day 26. Blood was collected into potassium-ethylene diamine tetra-acetic acid (K_3EDTA)-anticoagulant tubes and maintained on wet ice. Samples were centrifuged and plasma stored at −60 to −80°C until analysis (performed in singlet). Blood for clinical chemistry was collected from nonfasted animals under isoflurane via orbital sinus on day 28 of the dosing phase. Blood was collected into serum separator tubes (without anticoagulant) and allowed to clot at ambient temperature. Samples were centrifuged within 1 h of collection and serum was stored at −60 to −80°C, until analysis.

A macroscopic examination of the external features of the carcass; external body orifices; abdominal, thoracic, and cranial cavities; organs; and tissues was performed. Organ weights were recorded at the scheduled sacrifice.

Effects of SAR441255 on body weight in obese, diabetic cynomolgus monkeys

The effects of SAR441255 on body weight change was studied in male obese, insulin resistant and diabetic cynomolgus monkeys (*Macaca fascicularis*) and compared with a monkey-specific dual GLP-1R/GCGR agonist (Elvert et al., 2018b), another triple GLP-1/GIP/GCG agonist peptide 12 (Evers et al., 2020) and vehicle. The study was conducted over 16 weeks and included a 1-week selection period; a 3-week training and acclimatization period; a 2-week run-in period; a ∼1.5-week dose escalation period; a ∼4.5-week dosing period; a 1 week run-out period; and, a 4-week washout period (Evers et al., 2020).

Monkeys on a high fat diet (HFD) for > 8 months were screened to identify those animals to be used in the treatment phase of the study. Included monkeys were required to fulfil the following criteria: age > 8 years, body weight of > 8 kg, fasting glucose > 110 mg/dL, fasting insulin > 70 uU/mL, and normal complete blood count (CBC), liver and kidney function. Animals underwent training for 3 weeks to acclimatize them to the experimental procedures involving blood collection and administration of the study treatment. The training included single cage housing, in-cage arm presentation training, venipuncture desensitization without sedation, s.c. dosing (saline), bottled water intake training, and food rewards for each training session. Procedures initiated during the training period included twice daily cage-side clinical observation, daily measurement of food and water intake and weekly body weight measurement.

Following this, a 2-week run-in period was used for basal metabolic profiling (including measurement of plasma glucose, insulin, fibroblast growth factor 21 (FGF-21), total ketone bodies [T-Ket], 3-hydroxybutyrate [3-HB], triglyceride [TG], total cholesterol [T-C], low density lipoprotein cholesterol [LDL-C], high density lipoprotein cholesterol [HDL-C], glycated hemoglobin A1c [HbA1c], and non-esterified fatty acids [NEFA]), safety blood sampling (anti-drug antibodies [ADA], herpes B and measles virus by polymerase chain reaction [PCR]), an intravenous glucose tolerance test [ivGTT], daily s.c. dosing using normal saline (0.1 mL/kg), while the training procedure was continued.

Glucose, TG, and total-, HDL- and LDL-C, T-Ket and 3-HB concentrations in plasma were measured on a C311 or C501 biochemical analyzer (Roche Diagnostics, Mannheim, Germany). Plasma insulin concentrations were measured on a Cobas e411 Immunology analyzer (Roche Diagnostics) and plasma FGF-21 concentrations were measured by ELISA (Millipore).

The ivGTT performed during the run-in period was conducted with the animal under sedation with intramuscular [IM] injections of ketamine hydrochloride [HCl] (Bela-Pharm, Germany, 10 mg/kg). Following a 16 h overnight fast, the animals received an intravenous (IV) glucose bolus (0.5 g/kg, as 50% glucose solution (Sigma) over 30 s into the saphenous vein or a suitable peripheral vein based on the following dose calculation: Volume (mL) of 50% glucose solution = body weight [BW] (kg) x 0.5 (g/kg) / 0.5 (g/mL) or 1 mL/kg). Venous blood samples (~1 mL) for measurement of glucose and insulin levels were collected in pre-chilled K_2EDTA tubes pre-dose (0 min) and at 1, 3, 5, 10, 20, 40 and 60 min after completion of the bolus glucose injection. Samples were centrifuged within 30 min of collection.

At the end of the run-in period, the selected monkeys were randomly assigned to one of four dose groups (10 animals each) based on their bodyweight, total energy intake and their glucose/insulin exposure (area under the plasma concentration-time curve [AUC]) results from the ivGTT.

The test compounds (SAR441255, peptide 12, and the monkey-specific dual GLP-1R/GCGR agonist) and vehicle (PBS solution, pH 7.5) were administered to the alert/non-sedated animals as a once-daily s.c. injection in-cage between 10:30 (after breakfast) and 11:30 am over the 6-week dosing period (2 weeks dose-escalation phase, 4-weeks dosing phase on high maintenance dose) according to the assigned dose groups. The test compounds were formulated on the days of dosing in a PBS solution, at pH 7.5.

The dosing for SAR441255 was increased employing four steps every three days: 3, 5, 8, 11 μg/kg. The dosing of peptide 12 and the dual GLP-1R/GCGR agonist were increased within the same time interval: 3, 5, 8, 10 μg/kg and 1, 2, 3, 4 μg/kg, respectively. For the monkeys with relatively lower total energy intake, individualized dose designs were applied. Monkeys with food supplementation for one or more consecutive days were excluded from dosing and from the study.

During the entire dosing period, food and water intake was monitored daily and body weight was measured every 3 to 4 days. Venous blood samples for safety profiling (aspartate aminotransferase [AST], alanine aminotransferase [ALT], alkaline phosphatase [ALP], creatinine [Cr], blood urea nitrogen [BUN]) and CBC, pharmacokinetic profile, and metabolic profiling (as described above) were collected weekly; safety profiling (AST, ALT, ALP, Cr, BUN) and CBC: bi-weekly; glucose and insulin profiling, including T-Ket, and 3-HB, was performed throughout the study. Blood samples for pharmacokinetic sampling were collected on sampling days before and 1, 2, 4, 8 and 22 h post-dosing in all groups.

AST, ALT, ALP, Cr, and BUN concentrations in plasma were measured on a Roche C311 or C501 biochemical analyzer (Roche Diagnostics). CBC in plasma was measured on a Sysmex XT 2000i analyzer (Sysmex, Norderstedt, Germany).

After the dosing period, the animals underwent a 1-week run-out period in which dosing was continued and metabolic parameters were monitored to compare with baseline values. A further ivGTT was performed on day 45.

A 4-week washout period with continued observations then followed to monitor recovery. During this period, blood samples were collected for metabolic profiling (as described above), safety profiling and CBC, ADA samples, and herpes B and measles virus by PCR.

For analysis, 3 animals per test treatment group were excluded due to food supplementation for one or more days during the study period.

PET imaging and analysis in lean cynomolgus monkeys

Gallium-68 radiolabeling of [^{68}Ga]Ga-DO3A-Exendin-4 (Selvaraju et al., 2013; Velikyan et al., 2017) and the GCGR PET Tracer [^{68}Ga]Ga-DO3A-Tuna-2 (Velikyan et al., 2019; Wagner et al., 2020) was performed as described previously.

The radiochemical purity was over 90% (n = 23) with no unknown impurity of over 5%. Molar activity values varied depending on the age of the generator and were, on average, 43.1 ± 14.6 MBq/nmol (n = 23) and 33.4 ± 9.9 MBq/nmol (n = 23), respectively for [^{68}Ga]Ga-DO3A-Tuna-2 and [^{68}Ga]Ga-DO3A-Exendin-4 (range 13-67 MBq/nmol) at the end of the synthesis. The reproducibility was high with non-decay corrected radiochemical yield of 45.2 ± 2.5% (n = 23) and 41.6 ± 2.1% (n = 23), respectively for [^{68}Ga]Ga-DO3A-Tuna-2 and [^{68}Ga]Ga-DO3A-Exendin-4 and a success rate of 100%.

PET-CT imaging was performed in 3 female cynomolgus monkeys (weight 4.6 ± 0.9, range 3.8–5.8 kg), which were housed in the Astrid Fagraeus Laboratory at the Karolinska Institutet, Solna, Sweden. They were transported to the PET facility of Uppsala University Hospital on the morning of each experiment. Anesthesia was induced by intramuscular injection of ketamine HCl (10 mg/kg) at the housing facility prior to transportation. Venous catheters were placed in each leg for IV anesthesia, PET tracer administration, study drug administration, blood sampling and measurements of radioactivity. Following endotracheal intubation at the PET center, anesthesia was maintained with a mixture of 1%–4% sevoflurane (AbbVie), oxygen, and medical air. Body temperature was maintained throughout the examination by a Bair Hugger warming unit (Arizant Healthcare). Body temperature, ECG, heart rate, respiratory rate, oxygen saturation, blood pressure and glucose were monitored throughout the experiments. Fluid balance was maintained by a continuous infusion of saline or Ringer's acetate and supplemented with glucose if required.

Receptor occupancy studies were performed by PET-CT at the PET facility of Uppsala University Hospital, using tracer parameters optimized in prior dose escalation studies (Eriksson et al., 2019). Each animal was examined with one of two tracers ([^{68}Ga]Ga-DO3A-Exendin-4 or [^{68}Ga]Ga-DO3A-Tuna-2) on separate study days, at least 6 weeks apart. Two dynamic PET-CT scans were performed on each dosing day. Animals were positioned to include the abdomen in the field of view (FOV) of a PET-CT scanner (Discovery MI, 15 cm FOV, approximately 5 mm resolution, GE Healthcare) by assistance of a low dose CT scout view (140 kV, 10 mAs). Attenuation correction was acquired by a 140 kV, Auto mA 10-80 mA CT examination. Dynamic PET measurements were acquired over 90 min in list mode.

In the morning, a baseline PET-CT dynamic examination over 90 min was performed for measurement of GCGR or GLP-1R occupancy. The PET tracer ([^{68}Ga]Ga-DO3A-Tuna-2, [^{68}Ga]Ga-DO3A-Exendin-4) was administered IV in radioactive levels corresponding to approximately 0.05 μg/kg or less peptide mass. Peptide doses at this level were previously shown in dose escalation studies (Eriksson et al., 2019) to induce minimal or negligible receptor occupancy by itself (e.g., no mass effect), thereby fulfilling the tracer requirement (< 5% occupancy induced by radiotracer alone). Table S5 shows the administered radioactivity and peptide mass for each PET examination for each monkey.

After the baseline PET examination, s.c. 11 μg/kg SAR441255 (in PBS) was administered to each monkey. Two h post-dose (corresponding to the ~C_{max} of SAR441255), a second 90 min dynamic PET examination was performed in an identical manner with the tracer again administered at radioactive levels corresponding to negligible mass effect to avoid significant receptor occupancy induced by the radiotracer itself. This second PET examination investigated the changes in tissue binding (pancreas for GLP-1R and liver for GCGR, respectively) following SAR441255 treatment.

Image processing was performed according to standard optimized procedures for the PET scanner. The PET list mode data were reconstructed into 33 frames (12 × 10 s, 6 × 30 s, 5 × 120 s, 5 × 300 s, 5 × 600 s). Image acquisition was performed in three dimensions (3D) and reconstructed using an iterative Q-Clear 200 algorithm.

PET images were analyzed using PMOD 3.7 software (PMOD Technologies). Regions of Interest (ROIs) were segmented on transaxial PET projections assisted by accompanying CT scan images if available. Tissues were segmented on transaxial projections and combined into Volumes of Interest (VOI). For the liver, the portal vein and the vena cava were excluded by assistance of CT, as well as comparison of early and late image summations.

To determine an image-derived arterial input function, single pixel ROIs were placed in the aorta to avoid partial volume effects. There was no or minimal movement of the monkey during the day, as the body was fixated in a bear hugger.

The dynamic PET measurements were expressed as Standardized Uptake Values (SUV). Graphical analysis as described by Logan and colleagues (Logan et al., 1990) was applied to the PET dynamic data from the pancreas or liver and analyzed using PMOD 3.7 software (PKIN module, PMOD Technologies). Volume of Distribution (V_t) was calculated using image-derived aortic curves as input. The aortic input curve was corrected for the plasma-to-whole blood ratios obtained from blood sampling during each experiment. The aortic input curve was also corrected for the metabolic stability, i.e., the percentage of native [^{68}Ga]Ga-DO3A-Exendin-4 or [^{68}Ga]Ga-DO3A-Tuna-2 remaining in the blood, based on a population estimate determined in previous PET studies in cynomolgus monkeys. Goodness of fit for the model fitting was performed in the PKIN module (PMOD Technologies) using the standard assessments including Chi^2, Sum-of-squares and R^2. Individual V_t results for each scan are shown in Table S5.

Cardiovascular safety of SAR441255 in lean telemetered cynomolgus monkeys

The effect of SAR441255 on cardiovascular function was studied in freely moving conscious telemetered cynomolgus monkeys (*Macaca fascicularis*). The study included a 3-week acclimatization period, insertion of a telemetry device under general anesthesia, a 2-week recovery period, and then 4 experimental sessions separated by a 1-week washout period. Each experimental session included 4-days of repeated s.c. administration of study treatment (SAR441255 or vehicle control) followed by a 1-day recovery period. Thereafter, animals returned to the animal room for one week.

Selected conscious freely moving monkeys (n = 6, 4 males and 2 females, 3.12 to 6.10 kg body weight and 37 to 51 months old at the first experimental session) were randomly assigned to s.c. once daily vehicle (aqueous solution of 2.5% Glycerol (w/w) / 0.3% L-Methionine (w/w) / 0.09% Glacial acetic acid (w/w) / 0.02% aqueous solution polysorbate 20 (PS20) at 10% (w/w) adjusted to pH 4.5), or SAR441255 at 3, 30 and 300 μg/kg/day (dosing volume 0.3 or 0.5 mL/kg) over a 4-day period as solutions in control article according to a cross-over design (one dose by session for 4 successive days of dosing from day 1 to day 4) with a washout period of one week between each session. Arterial blood pressure (systolic, diastolic, and mean), heart rate (beats per min), ECG parameters and body temperature were continuously recorded on day 1 over 24 h post-dosing and on day 4 over 48 h post-dosing via the implanted telemetry unit [Data Sciences International). Measurements were collected every 15 min from at least 2 h prior to administration of SAR441255 (or vehicle) each morning (11:00).

Phase 1 study in healthy lean-to-overweight subjects

Trial design

In this first-in-human, double-blind, placebo-controlled study, participants were randomly assigned to receive single ascending s.c. doses of SAR441255 or placebo in a ratio of 2:6 (placebo [n = 2], SAR441255 [n = 6]). The originally planned doses were 3, 9, 20, 40, 60, and 75 μg to be administered in 6 cohorts (with the addition of an optional seventh cohort). Following analysis of measured plasma levels of SAR441255 in subjects receiving 3, 9, and 20 μg doses (first 3 cohorts) suggesting exposure was lower than initially predicted, the dose levels of cohorts 5 and 6 were increased and a seventh dose cohort added to better assess the adverse event (AE) profile at higher doses. The revised dose escalation plan for SAR441255 was 3, 9, 20, 40, 80, 150, and 250 μg.

Participants were confined in the clinical research unit during the whole treatment period from the day before dosing (day –1) until 4 days (cohort 1 to 4) or 3 days (cohort 5 and 6) after SAR441255 or placebo administration. Completeness of meal intake was monitored and recorded.

In total, 48 participants received single doses of SAR441255 ranging from 3 to 150 μg in 6 cohorts. Table S6 shows the baseline characteristics (day −1) of participants enrolled in the trial.

Trial medication and endpoints

SAR441255 or matching placebo were administered in the morning (fasting) by s.c. injection in the abdomen of the subject. The primary endpoint was safety and tolerability of single s.c. doses of SAR441255. Secondary endpoints included various pharmacokinetic parameters, and the pharmacodynamic endpoints of change in glucose, insulin, and C-peptide before and after a mixed meal test (MTT). Exploratory secondary endpoints included change from baseline in AA concentrations before and after the MMT, and plasma concentrations of C-terminal telopeptide of type I collagen (CTX) before and after SAR441255 administration.

Mixed meal test

The mixed meal consisted of an energy bar (e.g., Powerbar Protein Snack Bar, Peanut Butter Caramel 50 g) containing ~200 kcal (composed of ~23 g carbohydrates, ~12 g proteins and ~9 g fat) and a 430 mL liquid energy drink (e.g., Ensure Plus Therapeutic Nutrition Drink, Abbott) containing ~600 kcal (~92 g carbohydrate, ~24 g protein and ~20 g fat). The meal was given 8 h (cohorts 1 to 4) or 3 h (cohorts 5 and 6) after administration of study drug (day 1) and at the corresponding time at baseline (day –1).

The MMT was administered at the anticipated t_{max} of SAR441255 on the day of treatment (day 1) and corresponding time point at baseline. In cohorts 1 to 4 (3, 9, 20, and 40 μg doses), the meal was given 8 h after administration of the study drug at around 4 pm and at the corresponding time at baseline. Participants remained fasted for at least 4 h prior to the MMT (food and drink were not allowed except water and a light snack 4 h after dosing of the study drug). For cohorts 5 and 6 (80 and 150 μg doses), pharmacokinetic data from first 4 dose cohorts (1 to 4) showed that t_{max} occurred much earlier and therefore the MMT was given ~3 h after administration of the study drug (or at corresponding time point at baseline). Participants similarly remained under fasted conditions until the MMT, with a snack served at 3 pm (4 h after study drug administration or corresponding time point at baseline) and a dinner was served around 8 pm.

Safety evaluation

The safety and tolerability of SAR441255 was assessed by 12-lead ECG, vital signs, routine laboratory variables, 24 h Holter monitoring (baseline and day of dosing), physical examination, reporting of AEs and injection site reactions, level of antidrug antibodies (ADAs), and any episodes of hypoglycemia. ADA samples were collected pre- and post-dose and at 4-week (day 28 ± 3) follow-up. AEs were coded using Medical Dictionary for Regulatory Activities (MedDRA) version 21.1.

Blood samples and analysis

Venous blood samples were collected before and then at frequent times after dosing in each cohort; that is, every 30 min for the first 4 h, every 60 min from 5 to 10 h, every 120 min from 10 to 14 h and 22 to 24 h, and then at 28 and 32 h. All samples were centrifuged within 30 min of collection. Plasma was transferred to separate tubes, frozen immediately and stored at −80°C until analysis.

Plasma concentrations of SAR441255 were determined using a validated liquid chromatography-tandem mass spectrometry (LC-MS/MS) assay at Covance (Indianapolis, USA). Plasma concentrations within the validated concentration range (0.2-80 ng/mL) were used to calculate the pharmacokinetic parameters. The lower limit of quantification (LLOQ) was 0.2 ng/mL. Assessment for the presence of ADAs was performed in a Sanofi laboratory (Frankfurt, Germany) using an internally developed and validated enzyme-linked immunosorbent assay having a limit of detection (LOD) of 0.050 μg/mL.

Standard non-compartmental analysis was used to calculate the AUC up to the time of the last quantifiable concentration (AUC_{last}) and extrapolated to infinity (AUC_{inf}); percentage of the AUC extrapolated from the last observed time point (AUC_{extrap}); peak plasma concentrations (C_{max}); apparent total body clearance (CL/F); and terminal elimination half-life associated with the terminal slope ($t_{½z}$). Time to maximum plasma concentration (t_{max}) was reported as median values. For descriptive statistics of pharmacokinetic parameters, the arithmetic mean and standard deviation (SD) were reported.

The effect of SAR441255 on the plasma concentrations of selected exploratory biomarkers, including AAs and CTX, were assessed in cohorts 1, 2, 5 and 6, at baseline and at several time points post dosing (day 1).

Glucose concentration was measured enzymatically. Plasma insulin and C-peptide concentrations were measured by Electrochemiluminescence immunoassay (ECLIA). CTX concentration in plasma was determined using the Elecsys β-CrossLaps reagent (Roche Diagnostics) on a Cobas 6000 instrument equipped with a e601 module (Roche Diagnostics). The assay is a quantitative immunological test based on chemiluminescence readout. Analysis was performed according to the manufacturer's protocol with an LLOQ of 0.01 ng/mL. Quantitative AA analysis of the plasma samples was performed by LC-MS/MS at LabCorp (Burlington, North Carolina, USA).

QUANTIFICATION AND STATISTICAL ANALYSIS

Calculations

PET imaging and analysis

SUV were calculated as follows:

$$SUV\left(\frac{1}{1}\right) = \frac{Radioactivity_{tissue}(Bq)/Volume_{tissue}(cc)}{Radioactivity_{injected}(Bq)/\ Weight_{body}(g)}$$

Effects of SAR441255 on AAs

The treatment effect of SAR441255 on AA levels was investigated with the following linear mixed model as defined by the following equation:

$$\text{Biomarker} = \mu + \text{cohort} + \text{time point} + \text{cohort: time point} + (1\text{:subject}) + \varepsilon$$

with cohort, time point and interaction between cohort and time point as fixed terms and subject as a random factor. The placebo group and baseline (day −1) values were set as the reference groups.

Statistical analysis

Animal studies

Descriptive statistics [mean ± SEM] were used to summarize the measurement results. The measurement data taken at specified pre-treatment time points were designated as baseline values. Statistical tests were conducted for some parameters, as described in the respective figure legends. Treatment effects of SAR441255 were compared using one-way analysis of variance (AVOVA) or a two-way ANOVA followed by Dunnett's test for multiple comparisons of treatment effect versus the vehicle and obese control groups, respectively. A P value < 0.05 was considered statistically significant, and the level of significance was indicated. All analyses were performed using SAS version 9.4 (SAS Institute, NC, USA) under Linux via interface software EVERST@T v6.1.0.

Healthy subject phase 1 study

The sample size for this trial was based on empirical considerations. As the trial was an exploratory, first-in-human study with a small sample size, all pharmacokinetic, pharmacodynamic and safety parameters were analyzed descriptively.

Pharmacokinetic parameter estimates for SAR441255 were calculated using standard non-compartmental methods with PKDMS (inhouse software version 3.0 with Phoenix, version 1.4, Certara USA, Princeton, NJ) and SAS version 9.4 (SAS Institute).

Exploratory biomarkers were analyzed in the placebo (n = 4) cohort and the 80 and 150 μg dose cohorts (n = 6 in each). The dataset was checked for outliers prior to statistical analyses. Outliers were defined as observations that fell below Quartile 1 minus 3 times the interquartile range [IQR] or above Quartile 3 plus 3 times the IQR. No outliers were detected.

Each AA was centered to the mean value and scaled to the SD of the centered values. A heatmap representation of the data matrix was generated highlighting the visit and treatment arms for visualizing the global treatment effect on AAs. The profile for each biomarker was plotted as mean ± SEM by time point, colored by visit and shaped by cohort. The placebo group was not added to the plots to ease the readability. The treatment effect was further investigated using the linear mixed model described above.

ADDITIONAL RESOURCES

Clinical trial registry number NCT04521738: https://clinicaltrials.gov/ct2/show/NCT04521738